Graph Theoretic Analysis of The Human Brain's Functional Connectivity Alteration Due to Sleep Restriction

By

Marwa Antar

May, 2023

Director of Thesis: Dr. Sunghan Kim

Major Department: Engineering

ABSTRACT

Sleep plays a vital role in learning and memory consolidation. Several studies used brain models of sleep deprivation (SD) and insomnia to study the association between sleep deficiency and cognitive decline conditions. SD was found to cause similar, albeit subtle, cognitive decline symptoms displayed by dementia patients affecting attentional functions, decision making, working and long-term memory. This study examines the effect of sleep restriction (SR) on brain networks and utilizes Functional Connectivity (FC) analysis to identify patterns of information processing between different brain regions. It particularly applies weighted phase-lag index (wPLI) to quantify brain signals synchronization levels during a visual oddball paradigm task that evokes event-related potentials (ERPs) associated with face recognition. This study also examines the viability of graph theoretic analysis (GTA), which provides a holistic view on the brain network topology. GTA quantifies the brain connectivity features to assess the global efficiency and local efficiency of information processing, pre- and post- SR intervention. Significant alterations were found in all graph indices mainly in α-, μ- and β- frequency bands due to induced mental fatigue. The obtained results reveal significantly lower local connections ($p < 0.05$) and lower global efficiency ($p < 0.001$), particularly in the α- band as a result of mental fatigue, reflecting the impact of sleep loss on attention and memory processing.

Graph Theoretic Analysis of The Human Brain's Functional Connectivity Alteration Due to Sleep Restriction

A Thesis

Presented to the Faculty of the Department of Engineering

East Carolina University

In Partial Fulfillment of the Requirements for the Degree

Master of Science in Biomedical Engineering

By

Marwa Antar

May, 2023

Director of Thesis: Sunghan Kim, PhD

Thesis Committee Members:

Chris Mizelle, PhD

Loren Limberis, PhD

Graph Theoretic Analysis of The Human Brain's Functional Connectivity

Alteration Due to Sleep Restriction

By

Marwa Antar

APPROVED BY:

Director of Thesis _____

Sunghan Kim, PhD

Committee Member _____

Chris Mizelle, PhD

Committee Member _____

Loren Limberis, PhD

Chair of the Department of Engineering _____

Barbara Muller-Borer, PhD

Dean of the Graduate School _____

Kathleen Cox, PhD

TABLE OF CONTENTS

LIST OF TABLES

LIST OF FIGURES

LIST OF ABBREVAITIONS

Chapter 1. Introduction

Alzheimer's disease (AD) is the most prevalent type of dementia[1]. According to the World Health Organization's (WHO) reports, nearly 55 million people have dementia worldwide, with about 10 million new cases annually, and AD accounting for 60– 70% of the cases[2].

Dementia is a common disease in the elderly that's considered a major cause of disability and is now the 7th leading cause of mortality among all diseases worldwide[2]. Symptoms of Dementia include difficulties in memory, problem-solving, disturbance in language and comprehension, as well as general cognitive decline which is commonly preceded by changes in mood and behavior. Mild Cognitive Impairment (MCI) is considered early-stage dementia[3]. The first pathological mechanism that characterizes early-stage dementia is the accumulation of extracellular amyloid- β (Aβ) plaques [2] along with the abnormal intraneuronal tau protein expression that forms fibrillary tangles. Both pathological events occur in a progressive, exacerbating manner[1]. A previous study has shown that Aβ deposition can occur for decades before reaching the dementia stage, where the accumulation primarily begins in the precuneus, medial orbitofrontal cortex (mOFC) and posterior cingulate cortices (PCCs)[4]. Reduced functional connectivity in these brain regions has been linked to the build-up of Aβ during initial pathogenesis stage[4]. Multiple factors are linked to the elevated Aβ burden in the brain including genetic, environmental, age-related factors and numerous diseases such as diabetes[5]. Moreover, sleep disorders were found to have a substantial effect on AD pathogenesis[1].

Sleep plays a critical role in learning and memory consolidation[6]. Sleep alters the cellular structure of the brain and is crucial for the clearance of Aβ and other metabolic by-products[7]. Several studies used sleep deprived or insomniac subjects to study the association between sleep deficiency and cognitive decline conditions.

Findings demonstrated that sleep deprivation (SD) and insomnia may aggravate the progression of the disease and the symptoms severity and increase the likelihood of developing late-life cognitive impairment in healthy individuals[8]. Besides the long term effects of SD, Aβ accumulation was found to be a common feature in sleep deprivation and dementia[9], [10]. For instance, acute SD impacts Aβ burden in brain regions that have been involved in AD cognitive decline symptoms similar to those displayed by dementia patients, including attentional functions, decision making, working and long-term memory[11]. However, little have been documented on the functional connectivity level in affected brain regions due to insufficient sleep. This association between sleep deficiency and Aβ accumulation ought to have more attention in research.

Graph theoretic analysis (GTA) serves as an effective tool to quantify brain dysfunctions, as it uncovers instrumental information about the topological architecture of the human brain. This technique generally provides an in-depth analysis of the segregation in brain regions to perform more localized functions, and the integration of multiple networks to perform high level cognitive tasks associated with memory, attention and language skills[12]. More subtle changes might occur in cognitive abilities due to inadequate sleep compared to those resulting from dementia[9], [11], [13]. This urges the question of whether graph measures are capable of quantifying sleep deficiency-induced changes. This research aims to assess the viability of graph measures in quantifying the alterations in brain networks as a result of Sleep restriction (SR).

Chapter 2. Background

2.1. Cognitive Decline

Cognitive decline has been defined by the American Psychology Association (APA) as the reduction in one or more of an individual's cognitive functions including memory, decision making, awareness and mental acuity, most prevalent across the adult lifespan. The level of decline varies with the cognitive ability being measured. Fluid abilities, including abstract thinking, reason and problem solving, often exhibit greater declines than crystallized abilities [14].

Several factors are known to impact cognitive performance causing such declines including brain tumor treatment via radiotherapy and chemotherapy[15], psychostimulants and excessive alcohol consumption[16], [17] as well as the brain accumulation of Amyloid-β (Aβ). The physiological role of (Aβ) includes neural growth and repair, synaptic function regulation and supporting injury recovery. Biochemical alterations in Aβ molecules result in protein misfolding, which alters the protein structure and promotes the formation of Aβ plaques that accumulate within brain tissues, and is especially present in the extracellular matrix[18]. Aβ accumulation is one of two fundamental hallmark pathologies of Alzheimer's Disease (AD), the most prominent type of dementia[19].

2.2. Dementia

Dementia is a clinical syndrome caused by neurodegenerative disease such as AD, Lewy's body disease or the less prevalent cases of frontotemporal Dementia. Dementia is characterized by the impairment of multiple cognitive functions i.e., difficulties in memory, language, and challenges performing daily activities[19].

Aging is an important risk factor for all neurodegenerative diseases causing dementia, with AD being the most common type of dementia affecting 5–10% of people 65 years, and

50% of those over 85. Some risk factors for AD can be modifiable, such as having hypertension or diabetes, non-sufficient diet, and limited cognitive and/or physical activity. Other genetic-related are considered non-modifiable[19], such as carrying apolipoprotein E4 version of the (*APOE)* gene[20]. Progressive loss of memory is the main symptom of AD, as well as having difficulty learning new information, particularly autobiographical information, since AD mostly affects brain regions involved in episodic memory[21].

The loss of cognitive abilities occurs gradually, some cognitive functions might be affected by normal aging; however, cognitive decline might reach a transitional stage between normal aging impact and dementia, known as mild cognitive impairment (MCI). Although MCI symptoms' impact on daily activities seems trivial, it was found that those with MCI are at a significantly higher risk of developing dementia. Early diagnosis of MCI is favorable as preventative measures can slow down the progression of cognitive dysfunction[3].

Multiple approaches are used for the diagnosis of dementia, it's mostly diagnosed by patient's medical history, cognitive examination, laboratory tests and neuroimaging biomarkers.

2.3.Diagnostic Techniques

2.3.1. Cognitive Examination

The Mini-Mental State Examination (MMSE) and Montreal Cognitive Assessment (MoCA) are the most used screening instruments in clinical settings for diagnosing cognitive impairments i.e., MCI and AD. The diagnostic criteria in both tests are based on memory deficits, since it's the major symptom that MCI and AD have in common[22].

MMSE is a commonly used test to assess the cognitive functions among older adults, it includes tests of attention, word recall (memory), orientation, language, and visuospatial skills.

The evaluation is typically done by scoring 1 point on every question, with a few questions being scored out of 3 or 5 and are considered pivotal for the examination of cognitive abilities such as memory. Previous studies have emphasized the need to question its accuracy and sensitivity in Parkinson's Disease (PD); however, it is still used as the primary screening tool for cognitive impairment[22]. On the other hand, the Montreal Cognitive Assessment (MoCA) was developed as a brief screening instrument for MCI and AD. MoCA test includes 8 subtests similar to those in MMSE: visuospatial/executive, attention, naming, language, memory, abstraction, delayed recall, and orientation[23]. One point is added if the subject have completed ≤12 years of education[22]. Observations from a previous study indicated that The sections most instrumental in differentiating MCI from healthy subjects were the delayed recall, visuospatial and language sections, while those discriminating dementia from MCI were the visuospatial, orientation and attention sections[24]. Besides common questions in MMSE and MoCA, both tests are rated on a 30-point scale and the cutoff score is often modified depending on whether it's used for screening or in research settings[25].

The difference between MMSE and MoCA, however, lies in the complexity of the questions. MoCA has been shown to be more sensitive than the MMSE for the detection of MCI and AD in the general population. It's generally better suited for patients who might not currently have dementia nor cognitive impairment, but are at risk of their minor symptoms, while MMSE is considered a better test for more severe conditions[25]. The ability to modify the cutoff score provide flexibility for clinicians and researchers as it aids in data analysis and examination of certain changes in cognitive abilities over various pathological levels;

however, it makes such measures unreliable for diagnosis and especially susceptible to user errors.

2.3.2. Lab Tests

High concentration of amyloid-β (Aβ)1–42, and neurofibrillary tangles of phosphorylated tau protein are the histologic hallmarks of dementia and are used for diagnosis in laboratory tests, both biomarkers are quantified by analyzing blood samples or cerebrospinal fluid (CSF) samples obtained via a lumbar puncture. Multiple studies have compared the results of CSF biomarkers analysis of β--amyloid (Aβ1-42), phosphorylated tau, and total tau in CSF samples obtained from healthy subjects (control) and patients with different types of dementia to evaluate each biomarker's diagnostic accuracy as well as its capability of distinguishing AD dementia from other forms of dementia. Although CSF Aβ1-42 showed the highest sensitivity among other CSF biomarkers, none of the tested measures were reported to have a high specificity when it comes to discriminating AD from other types of dementia[26], [27].

2.3.3. Imaging Techniques

Multiple imaging modalities have been utilized to thoroughly examine the underlying etiology of cognitive impairment, which could be a chronic condition, such as that resulting from cortical and hippocampal atrophy as characterized in AD, or a curable symptom that stems from another neuropathological issue, like some types of tumors which might be cured after tumor resection; or normal pressure hydrocephalus which is relieved by different procedures. Currently used Neuroimaging biomarkers uses modalities that detect signal abnormalities, or measure the concentration of certain molecules in brain tissues[19].

Positron Emission Tomography (PET) has been widely used for the diagnosis of cancer, it has been a valuable tool in identifying the pathophysiologic mechanisms underlying

cognitive impairment, which aids in distinguishing AD from other causes of dementia such as Lewy's bodies and frontotemporal dementia by detecting the changes in glucose metabolism in brain tissues. This is possible due to the mechanism in which PET modality operates. This technique uses a radioactive substance (tracer) combined with a glucose-like substance. The compound is injected in a vein where it is carried through the bloodstream to the brain. PET modality captures the brain activity after the tracer have been absorbed by the brain tissues[28].

Functional magnetic resonance imaging (fMRI) is another competent technique that does not directly measure brain electrical activity, but rather relies on the blood oxygen level in brain tissues, indicating the intensity of neural activity. fMRI is known for its high spatial resolution, but it is not capable of recording changes in blood flow within brain tissues over a period of time[29].

Another technique has been widely used for dementia diagnosis is Electrocorticography (EcoG), also known as intracranial electroencephalography (iEEG), is an invasive technique that requires surgical placement of an intracranial electrode to record brain signals directly from the cerebral cortex, this technique is highly reliable for measuring brain activity as it is characterized by high signal to noise ratio[30]. However, non-invasive diagnostics are generally favorable. The non-invasive Electroencephalography (EEG) modality operates on the same principle and is used as an inexpensive means of analysis. Although the signal-to-noise ratio of EEG is not as high as that of ECoG, this technique plays a prominent role in research and clinical settings for its flexibility and high temporal resolution that enables clinicians and researchers to record brain activity over extended periods of time. EEG data require thorough processing before analysis; however, it is very well suited for the examination of conditions involving cognitive decline, which require special focus on the patient's response speed[31].

2.4. Sleep Deficiency

Sleep plays a critical role in learning and memory consolidation[6]. A significant correlation between sleep and memory extends to higher-order cognitive functions[32]. Sleep has crucial neurophysiological effects on the overall health of the brain, as it alters the brain's cellular oxidative state, which maintains neuroplasticity and cognition[33].

It's also crucial for the clearance of toxins and metabolic by-products from the brain, including Aβ and misfolded proteins via a special network of drainage vessels known as the glymphatic system[7], [34]. The glymphatic network tends to function more efficiently during sleep[1]. Many of these sleep-dependent functions were found to be sensitive to irregular sleep patterns and are therefore susceptible to disruption due to sleep disorders and sleep insufficiency in general. Sleep deprivation (SD) is a prevalent phenomenon in modern society that has been associated with poor cognitive and physical performance. Knowledge of SD effects on cognition in current literature is limited and are only beginning to be examined from a scientific perspective fairly recently[11]. However, there is a broad consensus that the failure to maintain good sleep hygiene i.e., inadequate sleep leads to a general neurocognitive slowing of response speed, alertness, and concentration.

Conditions resulting from sleep deficiency, including SD, are related to dementia in multiple ways; Studies have shown that insomnia and acute SD increase the likelihood of developing late-life cognitive impairment in healthy individuals[8]. Besides the long-term effect, sleep disturbance is one of many symptoms that individuals with dementia experience, it was also found to accelerate the progression of dementia and increase symptoms severity. One other way to look at this correlation is by considering the similarities between both conditions in terms of the underlying mechanisms as well as the cognitive deficits[9]. The trigger for Aβ protein misfolding remains controversial across studies. Most hypotheses revolve around the proteolytic cleavage of the amyloid protein precursor, where an alteration

in the enzymatic activity produces Aβ fragments that have a toxic effect on active neuronal cells[35]. Aβ accumulation and elevated brain protein tau were found to be common features in dementing conditions and sleep deprivation[1].

Increased Aβ accumulation was found in the subcortical region including the hippocampus after one night of sleep deprivation, which is considered among the highly sensitive brain regions to the neuropathology of the most common type of dementia i.e., Alzheimer Disease[9]. Aβ is normally secreted in the brain due to regular neural activity during wakefulness, this activity is inhibited during sleep, allowing the disposal of excess Aβ via the glymphatic network[35] A smaller increase in Aβ burden (~5%) from baseline was found after one night of sleep deprivation, compared to 21-43% increase in MCI and AD[9]. Suggesting that the difference in severity of the underlying mechanisms reflects more subtle changes in cognitive abilities due to SD compared to AD and MCI[9], [11], [13] The same imaging modalities have been used to examine these subtle changes, one of which is the EEG modality, which is considered favorable for its high temporal resolution, especially in cases related to cognitive decline as it is able to assertively detect variations in response latency[31].

2.5. Electroencephalogram EEG

Electroencephalography is a commonly used method that utilizes differential amplification principle to record electrical activity in the brain via small, metal discs (electrodes) attached to the scalp It provides safe and noninvasive approach to study psychophysiological correlates of healthy and impaired mental processes, and is essentially used to detect and measure brain waves over different frequency spectra: θ- band refers to the frequency components between 4 to 8Hz associated with deep stage of sleep; α- band ranging from 8 to 12Hz associated with a relaxed state of consciousness, passive attention, memory and focus; μ-band ranging from 12-13Hz and is associated with motor functions; and the

wide β- band ranging from 14-30Hz associated with alert consciousness and sensory processing including, attention, working memory and audiovisual integration [37].

The function of EEG is based upon neurophysiological principles; a special kind of neurons known as the pyramidal neurons are abundant in the cortical layer of the brain, where their apical dendrites extend through the cortical tissues. Both excitatory and inhibitory post synaptic potentials (EPSPs and IPSPs, respectively) are spread through the apical dendrites, reaching the surface of the scalp. The electric potential generated by neural populations can be modeled by small magnets (dipoles), where electric field lines flow conventionally from the negative to the positive direction. The dipolar currents simultaneously produce alternating voltages and magnetic fields significant enough to be detected non-invasively by multiple measurement instruments including EEG and magnetoencephalography (MEG), respectively[38]. Thus, EEG electrodes cannot detect the activity of individual neurons, it rather provides robust recordings of potential alterations over macroscopic brain regions. Over these macroscopic regions, a particular type of EEG known as time-locked EEG or event-related potentials (ERP) were used as a means to examine various cognitive functions, each could be monitored and assessed based on a specific ERP waveform that's known to be elicited in response to that function being executed[39].

2.6. Event-Related Potential ERP

Event-related potential (ERP) is composed of very small voltages that originate from neural networks in response to certain events or stimuli. When recorded, ERP waveforms indicate neural activity associated with sensory and cognitive processes[39] by reflecting the summation of postsynaptic potentials elicited in synchrony by a large number of pyramidal neurons within the cortical tissue while communicating and processing information.

2.6.1. ERP Waveforms

The resulting mean of recorded ERP components comprise a sequence of positive and negative deflections known as peaks, waveforms, or components. Each ERP component is elicited in response to a certain cognitive stimulus.

However, it remains difficult to determine the site of the ERP source simply by examining the distribution of voltage over the cortex. There are two broad categories of ERP components; the stimulus-dependent (exogenous) components that reflect automatic processing of external stimuli, and the cognitive (endogenous) components that reflect controlled processing and are independent of any external stimuli [40]. The name of an ERP component contains a letter (P or N) and a number, P and N are used to label positive and negative peaks. The number following P or N signifies the position of the peak in the waveform, also known as (Latency) which is also translated as the speed of stimulus classification or the time it takes the waveform to peak[41] as demonstrated in figure 1[42].

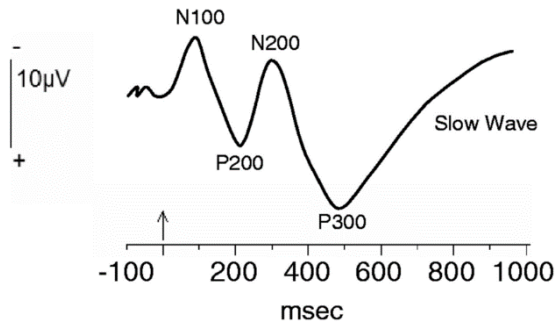

Figure 1: Schematic representation of ERP waveforms. Conventional plot of ERP waveforms where the negative voltages are pointing upward, and positive voltages are pointing downward. Labeling ERP components is based on positive P and negative N deflections [40] [41].

The appearance of each component in EEG recordings indicate the occurrence of a distinct neural activity associated with a sensory or cognitive function[43]. As previously mentioned, each ERP component is typically generated in certain brain regions. The simultaneous occurrence of such components give instrumental indications on how multiple

neural networks contribute to responding to certain events[41]. Examples of common ERP components that has been thoroughly investigated in the diagnosis of MCI and AD in literature and their indications are shown in table 1.

Table 1: ERP components and their significance

ERP	**Latency**	**Significance**
P1	Initial Peak	Exogenous response that is elicited by visual stimuli, such as luminance[44].
N170	~ 170 msec	Response to facial stimuli, reflecting a mechanism for human face detection. This component' amplitude is reduced in schizophrenia patients[44].
N200/N2	~200msec	It Consists of three components[45]: - **N2a:** Elicited by "oddball" paradigm, but it is mainly used in audition rather than vision. - **N2b:** Appears during heightened conscious attention to changes in stimulus. - **N2c:** Arises during classification tasks i.e., visual search tasks.
P200/P2	100-250 msec	- Signifies attentional recruitment and modulates perceptual processing. - N1/P2 component may reflect the sensation-seeking behavior[46].
N400/N4	250-500 msec	Response to words and other meaningful (or potentially meaningful) stimuli[47].
P300/P3	250-400 msec	Endogenous response. Like N2, it's a major component for auditory and visual stimulus. Elicited by the 'oddball' paradigm[45].
P600/P6	500-600 msec	Also called Syntactic Positive Shift (SPS), elicited when hearing or reading (i.e., auditory, and visual stimuli) grammatical or other syntactic errors. Often used in neuro-linguistical studies[45].

ERP components demonstrated in table 1 are known to represent the responses most affected by cognitive decline In AD and MCI subjects. Moreover, N200 (N2) and P300(P3) ERP components recorded from brain areas involved in the frontotemporal brain regions (involved with working memory) are of most interest in studies that assess changes in working memory due to total sleep deprivation (TSD). The amplitude of N2-P3 components

were found to decrease, and the latency was prolonged. After 36 hours of SD, another ERP component, P200 (P2) was found to increase in amplitude with a significant prolongation of latency. Thus, TSD can impair working memory capacity, which is characterized by lower amplitude and prolonged latency[35].

2.6.2. Time-Domain ERP analysis

Time domain analysis of ERP directly analyzes the amplitude and latency of individual components. It has been used as the fundamental tool to differentiate between healthy subjects and patients suffering from certain brain disorders, such as dementia or epilepsy. Shorter latencies imply faster response to stimuli and better mental performance compared to longer latencies[43], while larger amplitudes indicate more active brain response compared to smaller peaks. However, such analyses are rather complex as they are mainly performed in the time-domain, channel-by-channel. Single trials are known to have a poor signal-to-noise ratio, and high trial-to-trial variability, which explain possible inconsistent results across multiple studies on the same condition[48]. For instance, multiple studies have utilized this technique to analyze brain signals recorded from MCI and AD subjects. The significant variation in P300 component features between MCI/AD subjects and healthy controls is the point of agreement across the studies, particularly in the delayed latency after stimulus onset which was found to increase as the disease progresses[49]–[51]. However, only a few studies have found a notable reduction in the P300 amplitude in MCI and AD subjects[50], [52]. Since ERP time-domain analysis rely on analyzing single trials, it is also incapable of providing adequate information on subtle changes in the macroscopic brain network as a whole[48]. Functional connectivity (FC) analysis could overcome these disadvantages as it provides information about the communication between the distinct brain regions in a holistic manner[53]. More on functional connectivity measures and features is provided in the following section.

2.7. Functional Connectivity

Statistical measures can describe functional connectivity as the temporal correlations of spatially distant neurological events [53]. The theory of functional connectivity states that two brain regions elicit signals of a similar feature, either phase or power, as they exchange information. In other words, two regions are considered functionally connected if there is a statistical relationship between the measures of activity recorded from them[54], provided that the detected connection is noncausal. FC can be estimated through measures of correlation either in time domain or frequency domain [1].

FC measures have been generally used in a broad range of studies aiming to understand mechanisms of brain disorders. For instance, they have been calculated to identify abnormalities associated with schizophrenia and have shown augmented phase asynchrony in the β- and gamma frequencies[55].

FC measures provide a different approach to analyze ERPs holistically by evaluating the synchronization between different channels at different frequencies. This analytical approach can reveal network-wide alterations in the brain. It's important to pick the FC measure that is most instrumental for a given data set, depending on the required level of sensitivity and specificity.

Quantifying neuronal interactions remains challenging for several reasons. One reason is the overwhelming diversity of quantification methods of oscillatory interactions, which is often demonstrated with a substantial amount of technical detail, it's often hard to determine and justify the used method. One limitation of connectivity analysis is that the interpretation of the findings is not straightforward, the results are therefore susceptible to overinterpretation[56]. It's essential to highlight the fact that the conclusion about the strength of connection between two neural populations varies depending on the implemented measure to identify functional connectivity. Different approaches might

provide different results that describe the extent of the correlation between neural networks since each FC measure has different sensitivity and specificity issues [57]. FC measures are either power based or phase based.

Phase-based connectivity measures are used to estimate inter-site synchronization i.e., the amount of phase stability between two distinct signals over time. Several phase-based measures analyses including cross correlation, spectral coherence, phase lag index (PLI), and phase locking value (PLV) proved to be ultimately effective in assessing brain network connectivity.

2.7.1. Phase-based Measures

Phase measures are computed from the frequency domain representation of a pair of signals. The time-frequency transformation of epochs allows for obtaining the spectral representation of a signal composed of an amplitude and phase components of the oscillation. This combination is mathematically represented into Euler's form i.e., complex numbers ($Ae^{i\varphi}$) where A is the signal amplitude (real part) is represented as a vector that connects the non-zero point i.e., the value of the amplitude to the origin, and φ is the phase of the signal (imaginary part) that is represented by the angle this vector makes with the x-axis. This value can be graphically depicted as a point in the complex plane as (x+iy), where x represents the distance from the real axis to the non-zero point (amplitude value), and y is the distance from the imaginary axis to the non-zero point as illustrated in figure 2.

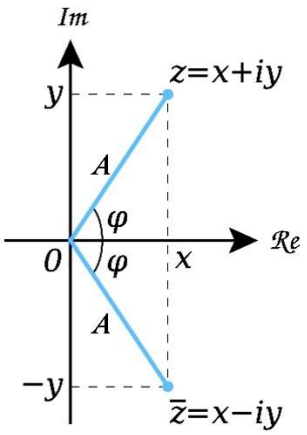

Figure 2: Representation of a complex signal and its conjugate in the complex plane. The lower blue vector $\bar{z}$ represents the conjugate obtained by taking the negative of the imaginary component of the original signal, i.e., upper vector z.

2.7.2. Cross correlation and Coherence

Cross-correlation was one of the earliest measures used to assess phase synchronization between two time domain signals[58]. Cross-correlation particularly based on Pearson's correlation coefficient and it measures linear connectivity via linear analysis of signal similarity, this is determined by what's known as sliding dot product of every point on a signal by every point on the other signal[56]. A major pitfall of this measure is that it does not account for the temporal structure of the signal, treats every point on a signal as a random variable. It's also used for linear connectivity and is useful for general applications involving similarity detection; however, neural signals are mostly bivariate and non-linear, which makes it hard to analyze brain signals to identify connectivity using this measure[56]. On the other hand, coherence, also referred to as the cross-spectral density is the spectral analysis of EEG signals. It's the frequency domain equivalent of the cross-correlation function. Coherence is calculated by the frequency-wise multiplication of a signal in frequency domain by the complex conjugate of another signal.

The conjugate is obtained by taking the negative of its imaginary component i.e., phase angle[56] as illustrated in figure 2 above, where (x+iy) becomes (x-iy).

The multiplication results in a point in the 2D cartesian axes where the vector represents the product of both signals magnitude, and the angle with the real axis represents the phase difference between them. The benefit of the coherence measure is that it's possible to obtain a good estimation of it in short segments of data[59]. Refer to figure 3.

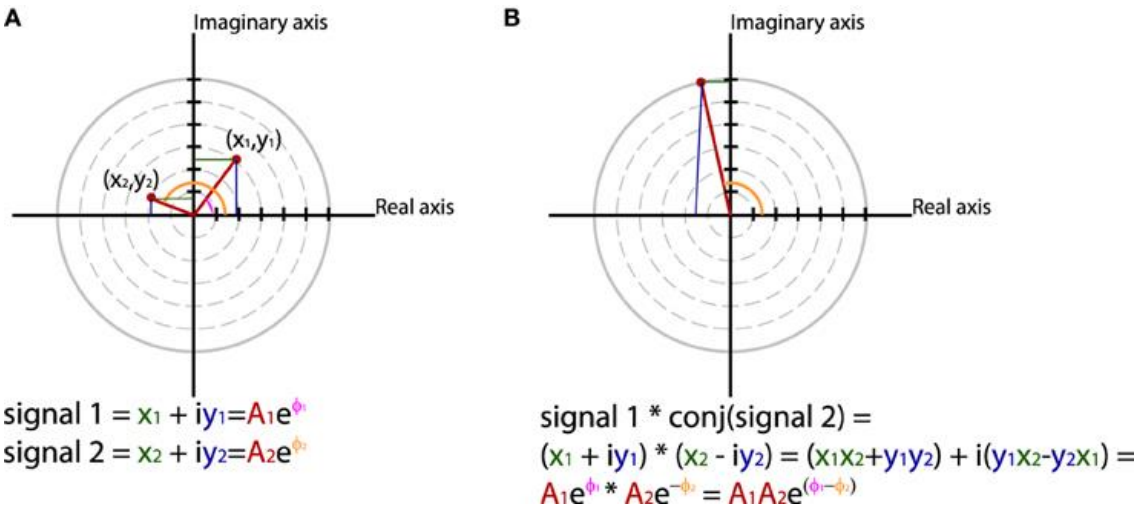

Figure 3: Frequency domain representation of signals A. The phase and amplitude components of two signals B. The cross-spectrum between a signal and the conjugate of another signal, where the vector length is the product of their amplitudes, and the angle is the phase difference between them [55].

Processing the signals in frequency domain might aid in averting from the temporal structure problem confronted in cross-correlation analyses; however, coherence measurements between recorded EEG signals might be impacted by two major caveats that complicate the process. One of which is the common reference problem, where fluctuation/noise resulting from the reference electrode contaminates multiple electrodes with the same voltage component, consequently indicating false connectivity between the regions over which they're attached[60]. In addition to the variety of computational methods to address such complication, assigning multiple references for the EEG electrodes significantly enhances the spatial scale where the connectivity is considered[61].

Volume conduction artifact can account for some patterns of synchronization. Since macroscopic potentials are projected to the electrodes attached to the scalp. Volume conduction is a common artifact in EEG and MEG recording that occurs due to one signal source being instantaneously projected towards multiple electrodes. The same field can also propagate through the head and skull tissues to adjacent electrodes, refer to figure 4. This artifact leads to misinterpretation of the data, as the result is attributable to a single source in the brain in what appears to be multiple distinct yet strongly and instantaneously synchronized signals from different regions i.e., electrodes. This yields false (spurious) indications of connectivity [62].

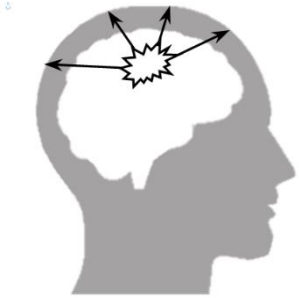

Figure 4: Illustration of volume conduction artifact. Multiple Electrodes can pick up on the same source activity, which could be misinterpreted as synchronized signals.

Besides instantaneous synchronization, with 0 phase between signals of interest is zero ‘0’, decreasing synchronization strength with increasing distance is another indication of possible spurious synchronization due to volume conduction while still having positive correlations between the projected signals in the frequency and time-frequency domains. It’s mostly positive in the time domain except for one case, where the electrodes pick up on the same signal but from opposite directions of the electric field (dipole). This is when the phase difference between the synchronized signals is equal to π.

There are multiple analysis approaches that can minimize or prevent the volume conduction artifact including the following:

1- Spatial filters such as the independent component analysis (ICA) Methods. ICA is a machine learning technique of data analysis that produce spatially localized and statistically independent subcomponents[63]. These methods aid in identifying mixed signals and separating them into independent subcomponents [64] refer to figure 5[65],

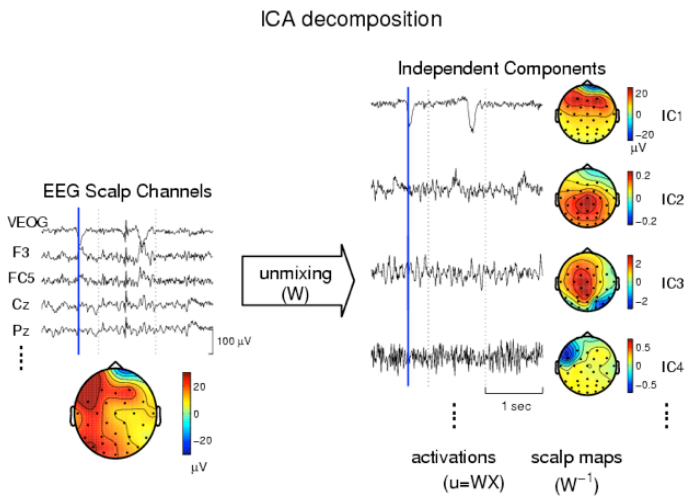

Figure 5: A schematic illustration of blind source separation using ICA techniques. The topographical map on the left shows the mixed signal before applying ICA. The maps on the right are the result of the unmixing process after applying ICA technique. This separation aids in identifying the source of every signal *[65]*.

2- Some phase-lag-based measures are insensitive to volume conduction activity. Those indices are widely used to eliminate the volume conduction artifact, unlike phase-clustering indices. The differences between them are further explained in the following sections.

2.7.3. Phase-Locking Value (PLV)

Phase-Locking Value (PLV) also known as Inter-Site Phase Clustering (ISPC) is mathematically defined as the absolute value of the average phase difference between two signals as shown in equation 1 below:

$$PLV = \left| n^{-1} \sum_{t=1}^{n} e^{i\left(\Phi^{j} - \Phi^{k}\right)_{t}} \right| \quad (1)$$

This measure is expressed as a complex unit length vector in the complex plane. Multiple vectors result from the two signals, i.e., phase differences between them at different time points is obtained. The clustering of these vectors in the complex plane gives an indication of the level of synchrony between the two signals[66], refer to figure 6[67]. Inter-site phase clustering is a good measure to use after the preprocessing stage to initially make sense of the amount of neural interactions one can expect from the data.

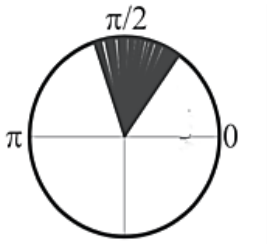

Figure 6: A Graphical Representation of inter-site phase clustering also known as phase-locking value (PLV) [67].

PLV can fail to detect real synchronization if phase angles differ across trials. It might also indicate spurious connectivity because it lacks the feature that can identify the effect of volume conduction. This issue can be further explained by introducing the following measure.

2.7.4. Phase Lag Index (PLI)

PLI measure estimates how distributed or clustered the phase variations are across multiple observations [55]. It differs from PLV in that it disregards phase locking indicated

by clusters of vectors) that are centered around the real axis (around 0, π, and 2π) on the unit circle. Having phase differences that are approaching zero is likely an indication of having two electrodes picking up on the same signal –due to volume conduction effect, which result in that signal being rejected using PLI measure, refer to figure 7[67]**.** The same applies to the phase difference of 2π. Moreover, it's possible that a phase difference of π is due to electrodes picking up on the same signal but from opposite directions of the dipole, which is also considered spurious connectivity. Note that this case will result in strong negative correlations in the timed domain. Using PLI eliminates spurious connectivity, but might as well ignore possible true neural interactions that just happen to occur simultaneously[68].

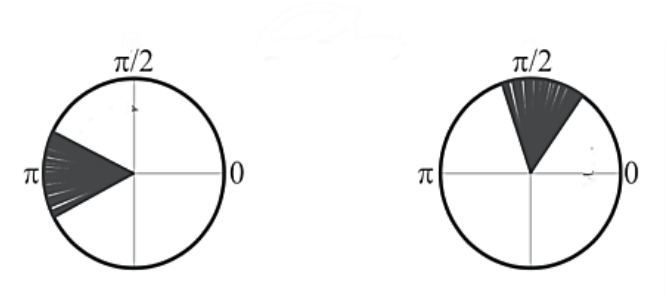

Figure 7: This figure demonstrates two cases that might occur by calculating PLI. The one on the left is a consistent phase difference that will be disregarded for being centered around the real axis, while the one on the right expresses strong phase locking index.

Phase-Lag Index is mathematically expressed in the following equation:

$$PLI = \left| n^{-1} \sum_{t=1}^{n} sgn(Im \left[e^{i(\Phi^j - \Phi^k)_t} \right]) \right| \qquad (2)$$

Both equations 1 and 2 are similar in that the phase differences between two signals over time represented in Euler's complex form. Those complex components are averaged, summed, and have their absolute value obtained. However, two additional transformations can be observed in equation 2: the first is in the symbol (Im) which projects the resulting phase differences vectors into the imaginary axis (a group of points along the vertical axis).

The second transformation is the (sgn) function, which stands for ‘sign’ referring to its location on the positive or negative parts of the vertical (imaginary) axis. This function converts the imaginary components into a group of unit vectors with values of -1’s and +1’s, which are summed and averaged to obtain the index. Obtaining PLI of 0 indicates instantaneous coupling, possibly due to volume conduction, while PLI of 1 is true interaction indicating functional correlation between the two neural network from which the two signals originate[68]. This process, particularly utilizing PLI, provides information on interregional neural communication with little to no false positive connectivity (type II errors).

2.7.5. Weighted Phase Lag Index (wPLI)

Despite its robustness against type II errors, A major caveat in PLI is that it can reject true positives of small phase differences approaching zero, as such cases are identified as spurious connectivity and are mostly eliminated. This is attributed to its sensitivity to noise and volume conduction that is hindered by the discontinuity occurring due to its calculation [69]. Consequently, small perturbations affect phase synchronization as they turn phase leads into lags, and vice versa. Another analysis method has been developed recently that would overcome these pitfalls known as the weighted phase-lag index (wPLI). Similar to PLI, this measure is obtained by calculating the cross-spectra’s imaginary components; however, it differs in that it weights the influence of the phase leads and lags by the imaginary component’s magnitude [69]. wPLI is represented by equation 3 shown below:

$$\Phi = \frac{|E\{|\Im\{X\}|sgn(\Im\{X\})\}|}{|E\{|\Im\{X\}|\}} \qquad (3)$$

Where $\Im\{X\}$ is the imaginary component of the cross-spectrum. The numerator demonstrates the scaling of the sign of the angle by the magnitude of the imaginary component. Thus, vectors that are further from the real axis (0 and π radians) have a larger effect on the estimated connectivity.

Moreover, the normalization in the denominator by the imaginary component's magnitude limits the impact of small perturbations and noises, which puts the cross-spectrum elements around the real axis at risk of altering their "true" sign, causing phase leading and lagging changes to them. Figure 8 demonstrates the difference between PLI and wPLI in estimating phase differences closer to the real axis.

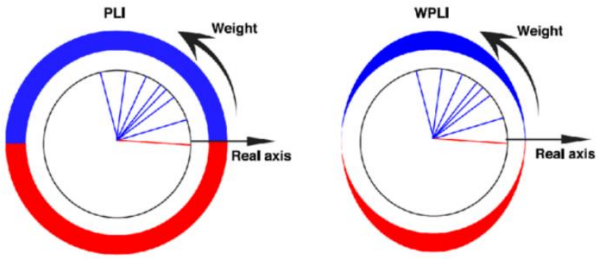

Figure 8: Illustration of (PLI) and weighted phase lag index (WPLI) -each blue line on the unit circle represents the phase differences between two signals. In PLI, each nonzero phase difference contributes equally to the synchronization value. In contrast, wPLI gives higher weights to vectors far from the real axis.

In other words, the components that are projected closer to the real axis are given the smallest weights. These changes are graphically represented as rotation of resulting vectors across the real axis, unlike PLI calculations that are very susceptible to the noise impact due to its complete dependence on the sign of the phase. wPLI seems to be preferred in data analysis, since it offers a high level of sensitivity and specificity while maintaining the maximum amount of data as demonstrated in several studies that utilize this measure instead of PLI[69].

2.8. Graph Theory

Besides quantifying phase synchronization levels using phase-based measures, extensive research has been conducted to develop techniques that model brain functional connectivity. The application of graph theoretical analysis on connectivity measurements has been broadly studied during the last decade, and has offered new insights into the structure and function of

the distinct brain networks[70] as well as identifying abnormalities that possibly indicate clinical disorders[71].

Graph analysis represents the brain topographically by illustrating a group of elements and their pairwise interconnections, also known as nodes (vertices) and edges (connections) where the nodes are the distinct neural elements, and the edges connect those nodes together indicating the level of synchronization between them at a certain time point. In their simplest form, the constructed nodes and edges are summarized in what's known as a connection matrix (adjacency matrix). The nodes are represented by the labels of the rows and columns in an n×n matrix, where n is the number of nodes. In weighted adjacency matrices, a link is represented by a zero or non-zero matrix element that varies depending on the strength of the connection between two nodes. After constructing the network and the adjacency matrix, many graph measures are quantified to assess the network topology and efficiency[71].

Weighted adjacency matrices can be directly used in quantifying graph measures. However, another step is commonly applied in the construction of the graph before evaluating its organization and features that involves thresholding of the matrix. The process of thresholding creates binary adjacency matrices which only include the set of edges with the largest weights that together form the graph. The absolute threshold and the proportional threshold are two of the most applied methods to perform adjacency matrices thresholding, each of which has a different influence on graph connections, particularly the weaker connections. For instance, when absolute threshold is applied to matrices, all connections that are weaker than a certain threshold value are set to 0. The elimination of weak connection is considered an advantage in this type of threshold, since weak connections highly impact the overall organization of the network. However, absolute thresholds are considered unreliable in comparing patient and control groups as the resulting network measures were generally unstable due to the inconsistent density (number of connections) [72].

The proportional threshold, on the other hand, avoids the systematic differences in the number of edges, as a percentage of strongest connections are selected to represent network edges, which maintains equal network density across graphs. This approach, however, introduces artifacts to the constructed network and derived graph indices attributed to the inclusion of less reliable connections to keep a consistent density across networks [73]. Many thresholding approaches of higher complexity are being developed to overcome these pitfalls and obtain the most informative connectivity values across the brain network. There is no consensus on the type of threshold to be used to obtain the representation closest to the anatomical network, especially when it comes to patient control studies where brain networks of control groups are compared with pathological conditions. For instance, different results can be inferred from the same graphs depending on the applied thresholding technique, which impacts the reproducibility of the results[74].

The quantification of network features utilizes different measures that can describe the topological graph on a global or nodal level. Global graph properties essentially quantify functional segregation of neural networks; integration between distant brain networks to process information; small world-ness –which refers to centrality; as well as assortativity referring to network resilience against failure.

2.8.1. Segregation

Segregation is a measure that describes the degree to which network nodes form localized communities that specialize in a certain task or process. Two measures are commonly used to quantify the level of segregation in brain networks as demonstrated in figure 9.A; clustering coefficient, which indicates local connectedness relative to one common node, i.e. considering one node, how many of its neighboring nodes are also connected to one another[12]. In brain networks, anatomically adjacent or functionally connected areas are generally considered modules[70].

The second measure of segregation quantifies the strength of division between these separate modules, and is called the modularity of a network [75]. Each module is comprised of a group of nodes that share high connectivity among each other i.e., similar degree.

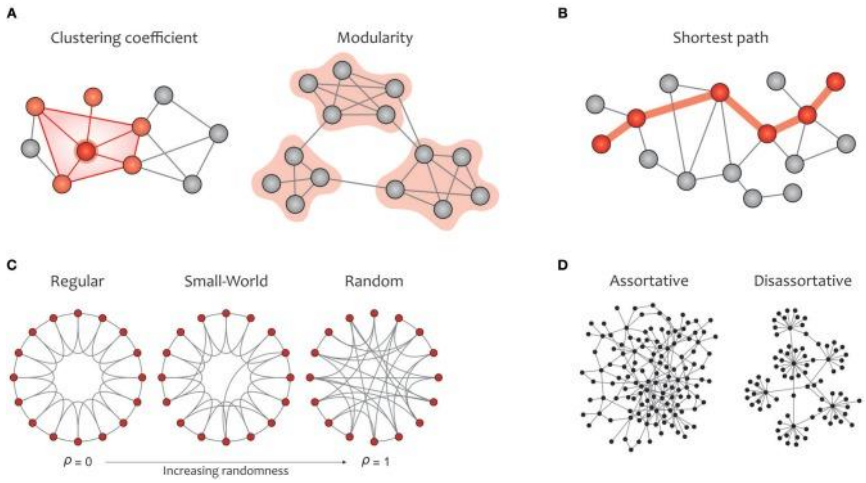

Figure 9: A schematic representation of the 4 global graph measures; part A represents the two fundamental properties of segregations i.e., clustering and modularity. Part B represents the integration in brain networks captured by path length. Part C represents the small world-ness. Finally, part D represents the level of network resilience against damage *[70]*.

2.8.2. Integration

Integration provides insight into the efficiency of information communication between the networks or the capability of distributed brain networks to rapidly combine specialized information to perform tasks of higher complexity. This capability is generally quantified by a measure termed as the characteristic path length as indicated in figure 9.B. Path length is the average distance between one node and all the other nodes. The shorter the path length between network modules, the higher the integration between them[12].

2.8.3. Centrality

The centrality (small world-ness) account for preceding properties of brain networks, representing the ideal balance between network segregation and integration. In other words, centrality is a parameter that describes the extent to which the network is optimizing information transfer by maximizing functional segregation while maintaining relatively short path length i.e., high global efficiency or integration level, refer to figure 9.C. Small world-ness is a critical concept that is indicative of both localized and global efficiency of information processing as both functions together contribute to changing the cognitive state.

Many centrality measures such as closeness and betweenness centrality, however, describe nodal-level features by identifying the most important –central nodes in the network, the importance of a node could be determined based on the number of connections it makes with adjacent nodes, or how often it lies on shortest path lengths between other nodes. Nodal centrality is dedicated to graphs of distant, non-neighboring clusters of nodes that are able to reach one another via the shortest possible path length[70] There are numerous centrality measures used to describes the importance of a node in a graph, by identifying provincial hubs that connect a group of nodes within the same module, as well as connector hubs, which connect multiple modules within a network as shown in figure 10. These indices include degree centrality, betweenness centrality, Eigenvector centrality and closeness centrality. All of which describe the nodes' significance based on different characteristics[76].

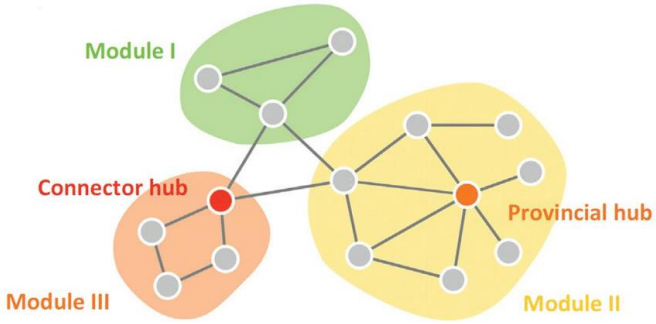

Figure 10: An Illustration of Provincial Vs. Connector Hubs [77]. A module consists of densely clustered nodes in a network. A provincial hub is the node that forms the largest number of connections with adjacent nodes, while a connector hub forms connections with other modules and contributes to the global efficiency of the network. Centrality measures can identify the extent to which each node contributes to global and local connections with all other nodes in the network.

Degree centrality is the most basic measure which captures the importance of a node based on the number of its edges as demonstrated in figure 10. Mathematically, it's described as the ratio between the total number of connections it has with other nodes to the number of all possible connections it could make[76]. This measure can only capture the importance of a node within its local module rather than an absolute measure of its significant within the network on a macro level, which is required to get a proper understanding of its overall degree centrality and influence[77].

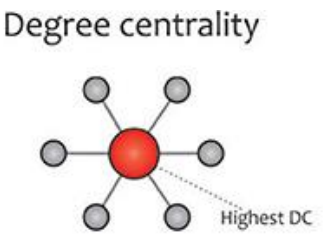

Figure 11: Degree centrality is defined as the number of a node's edges [70].

On the other hand, closeness centrality quantifies the closeness of one node to the other nodes in the network, which also indicate how fast the node can reach and communicate with other nodes. Closeness can be mathematically described as the reciprocal of the total distance between the node and all other nodes connected to it. The smaller the total difference the more central the node is[76].

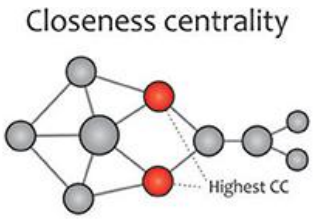

Figure 12: Closeness centrality is a measure of easy and fast access to other nodes [66].

Betweenness centrality describes how critical the node is in functioning as a connector or bridge between other groups of nodes.

It quantifies the number of times a node acts as a bridge along the shortest path length between two other nodes. In other words, nodes that have a high probability to occur along a randomly chosen shortest path between two nodes have a high betweenness value[76].

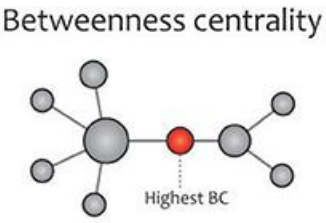

Figure 13:Betweenness describes the node's role as a bridge to separate modules [70].

Eigenvector Centrality, also known as prestige centrality, describes the significance of a node based on the significance of the nodes its connected to. This measure assigns relative scores to all nodes in the network based on the concept that connections to highly connected nodes contribute more than connections to nodes with low degrees of connectivity[77].

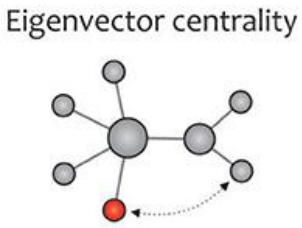

Figure 14: Eigenvector describes the significance of a node due to its connection with other significant nodes in the network rather than the number of connections [70].

There is no measure that's favorable to quantify the nodes' capacity to influence other nodes in the network. It all depends on the context i.e., the application or characteristic of most interest in the analysis of the distinct brain networks. Since this thesis project is concerned with the global features of networks describing the overall difference, many of the introduced centrality indices are beyond the scope of this study.

2.8.4. Assortativity

Highly connected nodes in a brain network –also known as hubs– result in the creation of local clusters. A network is classified as assortative or disassortative based on the level of nodes attachment to other nodes in the network that are similar in some way, mostly in terms of the node's degree as demonstrated in figure 9.D. Assortativity quantifies network resilience against random or deliberate damages in the main components that is, if one node fails to fulfil its task another node of similar function can take over and compensate for the deficiency. The level to which hub nodes contribute to the network resilience and its overall function is based on the participation coefficient, a hub node with a high participation coefficient is a connector hub, which interconnects nodes between different network

modules; and lower coefficient signifies a provincial hub that is responsible for linking nodes in the same module[70]. Degree assortativity measure of global networks typically ranges between −0.3 and 0.3[78]. The difference between modularity and assortativity is that the former is concerned with community detection in a network no matter the degree of connected nodes, while assortativity is concerned with nodes of similar degree connecting to each other.

This property is of great importance and is used to quantify the ability of a network to function in the presence of brain dysfunction caused by physical damage of brain tissues due to brain lesions or strokes, as well as dysfunction resulting from psychiatric disorders including epilepsy, AD and multiple sclerosis (MS). Very few studies have applied graph to investigate other disorders such as major depressive disorder (MDD) and obsessive-compulsive disorder (OCD) and insomnia, further research is required to better identify the brain network changes related to these disorders[70].

2.9.Graph Theoretic Analysis of Dementia

Graph theory measures have been used to assess the structural differences in brain networks. Changes in the brain due to neurodegenerative disorders have been of particular interest[79]. Graph theory has been applied to distinguish between brain networks in MCI, AD and healthy subjects.[80]. Multiple studies demonstrated similarities between the graph of the MCI group –early stages of disease- and AD group, which could also be distinguished from the healthy control groups. This suggests that cognitive network analysis may be a useful technique for characterizing differential cognitive profiles between different neurological populations not only in the dementia stages of disease but, furthermore, in the early stages[81], [82].

In one study, functional connectivity alterations in AD patients were only found in certain brain regions to the same extent, this suggests a heterogeneous disruption of the brain network. GTA of the FC data confirmed this idea, as it revealed lower normalized clustering coefficient in the lower α- and β- band and an increase in path length in the lower α- band in the AD patients group[83]. However, another study shown a significant increase in clustering coefficient across AD patient groups, while all patient groups revealed substantially higher integration when compared with healthy older adults, with AD patients having the highest global efficiency compared to the other patient groups [84].

The discrepancy in results across research studies suggests a rather unclear relationship between underlying neurophysiological changes in network topology and the variations seen at a cognitive level. The same study indicated different levels of modularity between healthy controls and AD and MCI patient groups. Considering language and memory cognitive domains, modularity was generally higher in patient groups compared to healthy older subjects, this demonstrates a major characteristics of AD which is the impairment of memory and language cognition [84].

Alterations were apparent in the centrality measure between the groups, betweenness centrality levels were distinctly lower in-patient groups compared to healthy controls in the domains of abstract reasoning and semantic processing. The same trend was observed when comparing AD group with MCI group, indicating that these two domains could be useful in characterizing the network alterations due to age-related neurodegeneration even in early stages of disease[84].

Cognitive impairment patients' reliance on crystallized semantic ability is drastically decreased due to neurodegenerative pathology. This particular domain is generally considered one of the earliest signs of cognitive impairment. Memory was shown to be an

inadequate domain to examine cognitive decline using betweenness centrality as very similar levels were found among patient groups as well as healthy older adults in semantic and episodic memory domains, where both had significantly lower averages compared to middle-aged adults. This is apparently due to the memory decline feature exhibited by these groups due to aging[84]. A study has been conducted on subjects under the influence of chronic sleep deprivation has reported similar trends in terms of segregation, integration and small world-ness, as well as a significantly lower assortativity compared to control networks[85].

Spurious connections have been an issue in identifying connectivity using graph theory across studies due to variations in thresholding of networks and the lack of standardized definition of nodes and edges to give biologically meaningful information[79]. Ongoing research is concerned with developing more plausible graph models and analytics to account for the instability and inconsistency in reported results across the studies to quantify the effects of cognitive impairment [12], [86], [87]; however, little has been documented on the sensitivity level of graph measures to quantify sleep deficiency-induced changes, that are very subtle, yet highly similar to these associated with cognitive impairment.

Chapter 3. Thesis Hypothesis and Significance

Graph theory-based measures provide solid representation of functional connectivity between the distinct brain networks and has been applied in data obtained from different imaging modalities including fMRI, PET, diffusion tensor imaging (DTI) as well as EEG [79]. This thesis aims to utilize EEG data in analyzing the functional connectivity between brain regions in subjects under the influence of sleep restriction (SR) and apply GTA to examine its sensitivity level in picking up on the subtle changes in brain networks due to sleep deficits. The hypothesis is stated as below:

The hypothesis is that One night of Sleep restriction can cause network level disturbance which can be monitored by Graph-Theoretic Analysis.

The ERP component of interest in this study is the P300, which is elicited in the process of face recognition. Numerous changes were observed in this component associated with cognitive decline conditions. For instance, the P300-prolonged latency is considered one of the early indicators of MCI, which reflects the difficulty recognizing familiar faces. Indeed, much more subtle change in P300 latency is expected to be observed in SR subjects. It's expected to observe network-level changes in subjects under the influence of SR. A healthy human brain is typically modeled as a small world network, representing a state of balance between global and local efficiency. This model is described with high global efficiency (shorter characteristic path length) and high local efficiency (quantified using the clustering coefficient in this study). Some changes in this state of balance are expected post-SR, indicating decreased performance and cognitive abilities. These changes are assessed by applying graph theoretic analysis to wPLI functional connectivity results instead of channel-by-channel comparison of wPLI results.

Chapter 4. Method

Multiple steps were required to test the research hypothesis; these steps include data collection, data processing, data analysis i.e., applying FC, GTA. and statistical analysis. Numerous steps were required to process the collected EEG data as will be explained in the following sections.

4.1. Subject recruitment

Eleven healthy college students between 18-27 years of age participated in the study. College students were chosen for this experiment since sleep restriction (SR) conditions required participants to be within walking distance from the lab to avoid driving under the influence of mental fatigue. The subjects were recruited based on the following inclusion criteria: (1) Normal sleep-wake cycle and good sleeping habits; at least 6.5 hrs. per day over the week prior to the experiment. (2) Normal vision with correction (3) Ability to be within walking distance from the lab on the day of the second screening to avoid driving. (4) No habit of smoking or heavy alcohol consumption; (5) No recent history of medication; (6) No recent history of acute infection; (7) No history of diabetes or any endocrine disorders; (8) No braided hair, as it will affect the quality of recorded EEG signals.

No specific criteria were set prior to collecting the normal control (NC) data. The subjects were restricted to 5 hours of sleep on the night before SR, 2nd EEG screening. The criteria of SR included the following: (1) The subjects must avoid napping during the days of the two screenings; (2) caffeine consumption in all forms e.g., coffee, tea, or energy drinks is strictly prohibited during the day of the experiment; and (3) Subjects shall maintain their regular level of physical activity during the day. Potential participants were asked to complete a short medical history questionnaire that helped to determine whether they are qualified for the study.

The study procedure, medical questionnaire and informed consent documents are approved by the University Medical Center Institutional Review Board (UMCIRB). All participants signed the informed consent in accordance with the Declaration of Helsinki. They were also provided with clear explanation and instructions of the experiment. Compensation for their participation was provided after completing all stages of the experiment.

4.2. Data collection

Data collection consisted of two parts, the first one is an online cognitive test which is the computer-based Psychomotor Vigilance Test (PVT) which measures the subjects' response speed to visual stimuli presented on a screen. This test objectively evaluates fatigue-related alterations in alertness related to sleep loss, extended wakefulness, and time on task[88]. This test was administered to assess the cognitive state of each subject prior to EEG recordings, which helped as an initial indication of the effect of SR on subjects. EEG recording is the second part of the data collection process and was performed twice by each subject to obtain the control and SR data sets. Control data was obtained on the first day of experiment, where no restrictions on the number of sleeping hours determined prior to the first EEG recording. Each subject was seated in a comfortable chair 1.46 meter away from a large screen (Dimensions), providing a field of vision of approximately 25°.

The g. SAHARA cap is placed on their head. The 32 electrodes are placed over the frontal, central, parietal, and occipital regions based on the 10/20 international system positioning with the reference and ground electrodes placed over the mastoid process behind the ears. The lights in the lab were turned off to promote sensory deprivation, and white noise was played to silence surrounding noise. Subjects were asked to remain still during the test, and to only blink between images, during the inter-stimulus interval (ISI) to avoid possible blinking artifacts.

Subjects were instructed to close their eyes for 10 to 30 seconds to ensure signal clarity before running the oddball paradigm test. The test is repeated 5 times in every EEG recording session for every subject. The collected EEG data is transferred to BCI2000, which is a software that presents the visual stimuli and stores the recorded EEG data. The test is designed to trigger multiple ERP components, including the one of interest in this study: P300 which is involved in attention, memory and face recognition. Two categories of visual stimuli are presented to each subject during EEG recording: familiar faces and random, face-like objects. Familiar faces include the faces of 3 well known people: Dwayne Johnson, Barack Obama, and Robert Downey Jr. The random objects include wall clocks, sunflowers, buttons, etc. Typical oddball paradigm tasks include familiar and unfamiliar faces; however, including random objects in lieu of unfamiliar faces ensures no false trigger of P300 would result from possible familiarity of unfamiliar faces after viewing them twice i.e., during control and SR EEG recording sessions.

Participants were instructed to tap their left finger on their lap at the sight of random objects and tap their right finger for familiar faces. The finger tapping response helps sustain the subject's attention over the duration of the test. Prior to the 2nd EEG screening, the subjects were allowed to get no more than 5 hours of sleep at night and to hold to the previously indicated restrictions during the day. After at least 8 hours of wakefulness, the second EEG session was performed to collect the SR data with the same online cognitive test (PVT) at the beginning of the session, as well as the process previously performed in the first recording session.

4.3. Pre-processing

Raw data was preprocessed using MATLAB via a built-in EEGLAB toolbox. A bandpass filter with cut-off frequencies of 1Hz and 13Hz, were applied to the data to remove unwanted noise, artifacts and DC offsets. The data is then segmented into epochs of 1100ms; with 100ms before stimulus onset, 200ms duration of stimulus onset and 800ms post stimulus.

Each subject had a total of 300 pieces of data recorded for both stimuli. Half of that (150 pieces) is control data and the other half is the SR data per subject. Only the EEG data recorded in response to familiar faces was of interest in this study. Those epochs were extracted and used to assess the changes in P300 components in control and SR conditions for each subject. This reduces the number of data pieces to 30 containing the P300 component. To reiterate, it's hypothesized that the small difference between both conditions will be noticeable in the final GTA result indicating lower segregation in local, neighboring nodes due to slightly lower wPLI, and higher global efficiency i.e. shorter path lengths in SR networks that are expected to be more random.

4.4.Time-domain Analysis

A total of 30 epochs was obtained for the target stimulus (familiar faces) from each subject; 15 of them are control epochs, and the rest are obtained from the second EEG recording under the effect of SR. The grand average of EEG epochs of each subject was obtained to create one averaged ERP waveform, control epochs and SR epochs are averaged separately. This is a crucial step to get well defined P300 waveforms, which cannot be obtained from individual epochs [40]. Due to EEG signals susceptibility to noise and external signal interference, a process known as manual trial rejection is done by visually inspecting each averaged epoch and excluding epochs with interfering noise and unwanted artifacts such as ECG signals, blinking and movement artifacts (EMG signals with notably larger peaks).

After ensuring the cleanliness and signal quality of Averaged ERPs, the waveforms are classified into two categories: control ERP waveforms and SR-induced ERP components, and are furtherly averaged within their respective category, which eventually gives two averaged ERP waveforms representing each category. Those waveforms are used to mark the duration where P300 occurred, this time period is used in specifying the data of interest in further analysis steps.

4.5. Functional Connectivity analysis

Calculations of the weighted phase lag index (wPLI) is done using a toolbox created by East Carolina University's Sensory-Motor Integration Lab (SMILe). Morlet wavelet transform in this toolbox is used to separate the obtained ERPs into their frequency components, followed by time-frequency analysis. The convolution of a complex Morlet wavelet with the pure time series signal (i.e., the ERPs) results in a complex (analytic) signal, where the phase information can be extracted at every time point.

The time-frequency transformation was used to calculate the cross-spectral data for each pair of channels, by multiplying every channel with the conjugate of the second channel. This process allows for the extraction of phase differences between signals at each time point in each frequency. A 5D matrix contained the time-frequency cross-spectrum information of two channels, frequency, time and trial in the data structure channel x channel x frequency x time x trials. Since connectivity results over time were of concern, down-sampling of the data was necessary to get connectivity results at specific time points (every 10ms) to facilitate comparison between phase synchronization level over the duration of a familiar face trial. The initial Sampling frequency was changed from 512 to a 100Hz, the former frequency resulted in 562 sample (50 before stimulus onset and 512 samples post stimulus), since each epoch consists of a pre-stimulus duration of 100ms in addition to the main trial, post-stimulus

epoch 1000 msec long. A total of 110 samples are obtained with the new sampling frequency. Having epochs of 1.1s, the total number of time points of interest, excluding 0, was 10 time points. The data was then separated into distinct frequency bands: delta (1-4Hz), θ- (4-8Hz), α- (8-13Hz), and β- (13-30Hz).

Data in every frequency band were averaged and consolidated in a 4D matrix of the structure of channel x channel x time x trials. Figure 15 represents the changes in the data structure after each step of the connectivity analysis.

wPLI was then calculated at each frequency band for a total of 15 epochs for every subject i.e., 15 trials. At each iteration, a Monte Carlo simulation was performed based on 75% of the trials randomly selected out of the 15 trials. The trials were averaged and used in the wPLI calculation. wPLI was calculated both per trial as well as per time in the same 4D matrix of two channels, time and trial. At that point, the output was the wPLI resulting from every pair of channels obtained over time for every single trial. wPLI was further averaged over all the trials, which results in a 4D matrix as an output with a data structure of channel x channel x time x stimulation. The resulting 4D matrices represent the average wPLI obtained from every pair of channels in a 32×32 matrix at each time point of interest. The P300 time period was specified using the grand average obtained from each of the two categories i.e., NC and SR based on the previously mentioned time- domain analysis step. Only the matrices of wPLI in the predetermined P300 time period will be considered for further analysis. The result is 10 control. 32-by-32 matrices, and 10 SR 32-by-32 matrices in each frequency band for every subject.

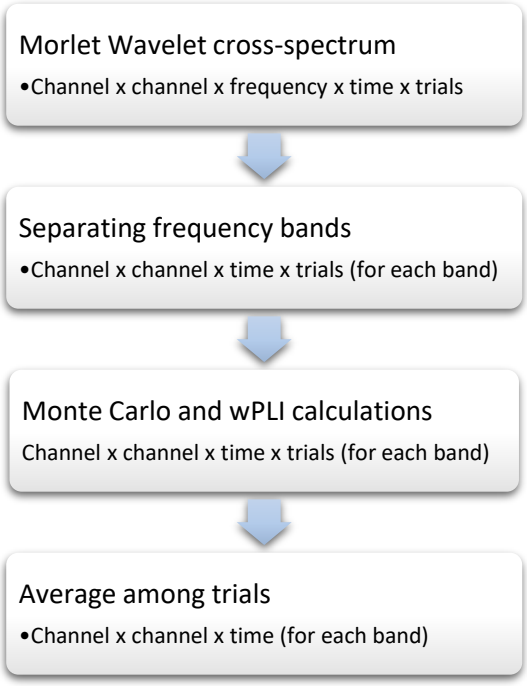

Figure 15: A representation of the data structure and matrix size along the process of FC analysis

4.6.Graph Theoretic Analysis

wPLI results were used to construct adjacency matrices of n x n x time x simulation. wPLI values range from 0 to 1 were considered the weights of the edges obtained over the period of the P300 component. Since this study one compares differences in cognitive states in the same sample, an absolute threshold of 50% was applied to construct the adjacency matrices, which completely eliminated unreliable connections and allowed for the comparison of edge density of networks pre- and post- induced mental fatigue. Adjacency matrices analyzed in this thesis were undirected, as causality was not assumed in the presented functional connectivity analysis. Multiple measures were quantified to characterize different aspects of the global brain connectivity in the control and SR brain networks in terms of the efficiency of information exchange.

First, the global efficiency is calculated by taking the inverse of the characteristic path length quantified using the following formula:

$$L = \frac{1}{n}\sum_i \frac{\sum_{j\neq i} d_{ij}}{(n-1)} \qquad (4)$$

The i and j denote the matrix row and column, respectively, where n is the total number of nodes in the graph, and d_{ij} is the shortest distance between nodes i and j. The numerator is the summation of the shortest path lengths of every node to all other nodes (also known as the Weiner index), divided by the total number of nodes n multiplied by nonzero distance values to all other nodes (n-1). This measure provides information on the extent to which the network is integrated i.e., how efficient communication across the overall network. The shorter the average path length, the higher the global efficiency, which indicates more integrated modules in a network.

In contrast, network segregation describes the specialized function of a specific module. Segregation can be evaluated using the clustering coefficient that is calculated using the following formula:

$$C_i = \frac{\sum_j \sum_k w_{ij}\, w_{jk}\, w_{ki}}{(\sum_j w_{ij})^2 - \sum_j w_{ij}^2} \qquad (5)$$

This formula represents the average local clustering coefficient, where *j* and *k are immediate neighboring nodes of i in the graph* and w_{ij}, w_{jk}, and w_{ik} are corresponding weights. It could also be described in different notation as the sum of clustering coefficients calculated for every node individually, averaged over the number of nodes present in the whole network. A network of low clustering coefficient and a relatively short average path length is considered a random network, in contrast, a highly clustered network with longer average path length is a regular, organized network.

Another segregation index is modularity, which is a statistic that quantifies the degree to which a network may be subdivided. The simplest formula for modularity measures the network ability to be divided into two communities i.e., a subset of graph node that are densely connected to each other and loosely connected to other nodes.

$$Q = \frac{1}{2m}\sum_{ij}\left[A_{ij} - \frac{k_i k_j}{2m}\right]\delta(c_i, c_j)$$

The subtraction term is the basic mathematical representation of the definition of the modularity formula, it's the difference between the number of edges connecting nodes in a graph and the possible connections that may form in a totally randomized network. k_i and k_j are the degrees of nodes i and j, respectively, the ratio of the nodal degrees to the total number of edges, 2m, is the probability of having an edge connecting both nodes i and j in a random network. This term is subtracted from the adjacency matrix A_{ij} that holds the actual number of edges between nodes i and j. c_i and c_j are the class of nodes i and j, respectively, the Kronecker delta term returns 1 when the classes are equal and 0 otherwise which will set the subtraction term to 0 for all nodes that are not of the same class. Calculating those values over the entire network result in modularity (Q) of the network [89].

Modularity ranges between -1 and +1, where a negative Q value indicates the presence of fewer edges between nodes within a community compared to a random network. In contrast, a positive Q means there are more edges between nodes in the same community compared to a random network. Moreover Q = 0 indicate a random network.

The balance between the two measures can be found in small world-ness, which include multiple measures that capture the centrality of nodes in the network. The simplest measure is the degree centrality.

The degree of a node $d(i)$is mathematically described as the values in the row corresponding to that node in the matrix, or the sum of the values in its column represented by the following formula, these values represent the number of edges connected to that node. Degree centrality is a measure of the normalized node degree expressed by the following formula:

$$C_d(i) = \frac{d(i)}{n-1} \quad (6)$$

The denominator is the normalization part which brings all the resulting values to the scale [0,1], the closer the value to 1, the higher the degree centrality of the node. As previously indicated, the summation of values obtained from the row corresponding to the node is equivalent to that obtained from the corresponding column, since the adjacency matrix of an undirected simple graph is symmetric. It's important to note that having the degree of the node in the numerator implies the node dependence on the adjacent nodes directly connected to it [90].

Assortativity might give a unique insight into the efficiency and robustness of a network. Assortativity describes the association of nodes of similar weights, mostly in terms of degrees that is, high degree nodes tend to be associate with other nodes of high degree as well, and low degree nodes are associate with other low degree nodes in the network[91]. Disassortativity is expressed when dissimilar nodes associate with each other, which negatively impacts the robustness of the network. For instance, the disruption in a high-degree node cannot be efficiently compensated by adjacent nodes of lower degree.

Assortativity index is simply measured using Pearson's correlation coefficient as represented in the formula[91].

$$r = \frac{\sum_{i=1}^{n}(X_i-\bar{X})(Y_i-\bar{Y})}{\sqrt{\sum_{i=1}^{n}(X_i-\bar{X})^2}\sqrt{\sum_{i=1}^{n}(Y_i-\bar{Y})^2}} \quad (9)$$

A positive correlation coefficient indicates the network exhibits assortativity, while a negative value indicates disassortativity. Values closer to zero describe networks that are rather neutral[91].

Since those measures were quantified for each matrix over the 1000 simulations, the resulting indices were averaged over the simulations to get the mean value of each network index at every time point in each frequency band.

4.7. Statistical Analysis

Group differences were analyzed using a paired t-test to assess the means in the applied global graph from control and SR matrices. A matched-paired t-test was appropriate for the two sets of data collected from the same group of subjects before and after SR intervention. Therefore, the groups were considered dependent. In other words, the differences are found for each condition by calculating the mean of a graph index obtained from each subject over time. This helped in testing whether the mean difference is nonzero, meaning that the mental fatigue condition significantly affected the brain network over the duration of a trial where P300 was triggered by the oddball task. Three assumptions were necessary to run this type of t-test. The first applies to the data collected for this study which indicates that the groups must be dependent, also referred to as 'paired', since analysis is applied to test the effect pre- and post-intervention for the same group. The second assumption is that the observations i.e., data from different pairs are independent, meaning that each subject is independent of the others in the same group [92].

The third assumption is either a large sample size, mostly greater than 30 sample, or the differences between the values in the two groups to be normally distributed [92].

Conclusions were drawn after running the test about the effect of the induced mental fatigue on the topological features of the brain network that were calculated as graph measures. Statistical tests were performed in terms of each graph index between control network and corresponding SR network at every timepoint for averaged NC and SR indices.

Chapter 5. Results

5.1. PVT Results

The subjects reported the number of hours of sleep and wakefulness before coming to the lab for the 2nd screening. Sleeping hours varied between 1hour and 30 minutes up to 5 hours, all participants held to the sleep restriction (SR) instructions for 8-10 hours before their visit. The psychomotor vigilance test (PVT) was used to assess the fatigue-related alterations in alertness due to sleep loss. The average response scores of most subjects were suboptimal (longer than 300 msec) even in the control condition, this might be due to the high sensitivity of the test to time differences, or the subjects' unfamiliarity with the test, which require some time to fully adjust to the test mode and speed. However, most subjects scored longer response time (lower alertness) during their 2nd screening as shown in table 2. The score is in msec representing the time between the stimulus display (random numbers) and the subject's response to them with a single click on the screen.

Table 2: PVT results in msec of response time for every subject in control condition, and under the influence of SR.

Subject #	**1st Screening: Avg response time**	**2nd Screening: Avg response time**
01	380 msec; Suboptimal	396 msec; Suboptimal
02	410 msec; Suboptimal	560 msec; Suboptimal
03	302 msec; Suboptimal	327 msec; Suboptimal
04	320 msec; Suboptimal	286 msec; Excellent vigilance and alertness
05	322 msec; Suboptimal	320 msec; Suboptimal
06	302 msec; Suboptimal	354 msec; Suboptimal
07	295 msec; Excellent vigilance and alertness	314 msec; Suboptimal
08	310 msec; Suboptimal	332 msec; suboptimal
09	313 msec; Suboptimal	332 msec; Suboptimal
10	289 msec; Excellent vigilance and alertness	295 msec; Excellent vigilance and alertness
11	313 msec; Suboptimal	407 msec; Suboptimal

5.2. Thresholding

An absolute threshold of 0.5 was applied to the weighted adjacency matrices which were assessed for differences in synchronization levels between networks pre- and post- SR intervention. Matrices were displayed at 300 msec in each frequency band and were compared with the proportional matrices. The difference in synchronization level was clearly observed in absolute adjacency matrices before and after SR after eliminating subthreshold, weak connections. Figure 16 illustrates the absolute threshold matrices.

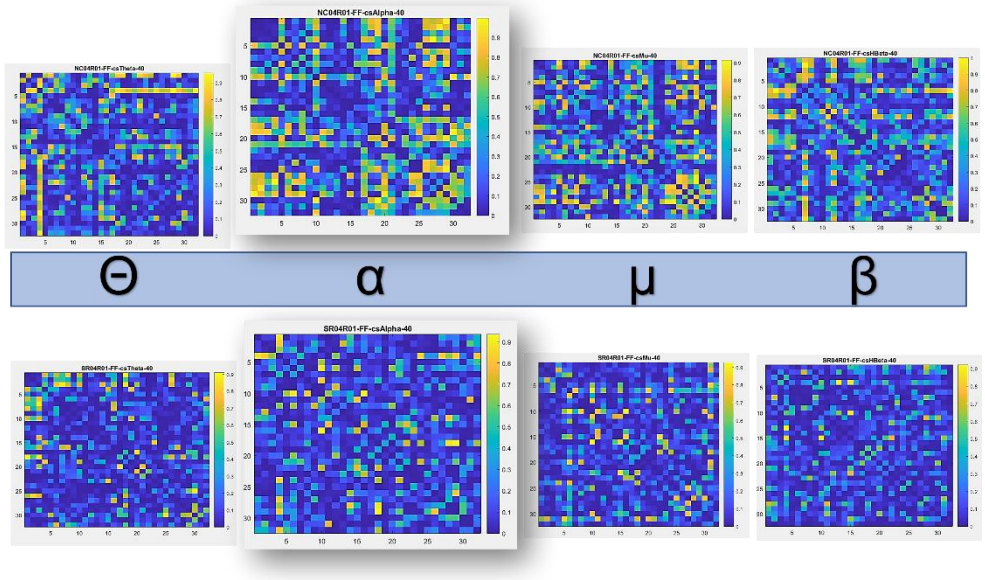

Figure 16: Adjacency matrices in different frequency bands at the peak of the P300 component, with absolute threshold applied. Top matrices are obtained from one subject's normal condition data, while the matrices below were obtained post SR. Higher synchronization levels were demonstrated in NC matrices compared to those in SR.

Higher synchronization levels, indicated in green and yellow pixels (0.5-0.9, respectively) were found in NC matrices compared to those in SR. A higher difference was observed in the α- band.

The constructed matrices of the α- band could be converted into topographic maps of nodes and edges to represent the brain network in the α- band. Figure 17 demonstrates this topology for the same subjects whose matrices are shown above.

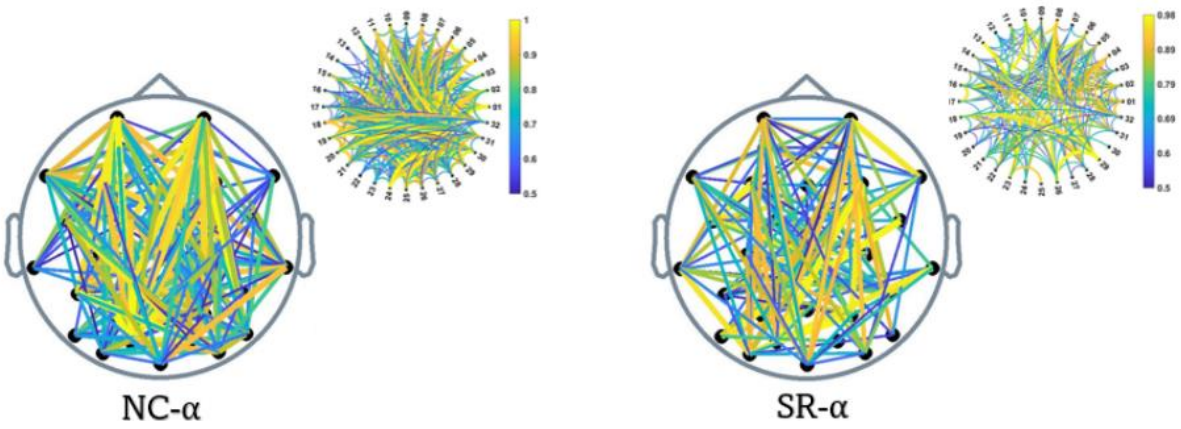

Figure 17: NC and SR brain topographic maps constructed from absolute-thresholded matrices at the peak of the P300. Weak connections below the threshold value (0.5) were eliminated. The connection density, as well as the edges weights in NC graphs are larger than those in the SR graphs.

The topographical maps could demonstrate the differences in the synchronization strength (thickness and color of the edges) as well as the graph densities, where more edges were eliminated from SR networks as a result of applying the absolute threshold of 0.5.

The previous figures depicted the qualitative differences between both conditions, which answers the question on whether there would be a clear change in the brain network under the influence of mental fatigue induced with SR. The second question to address was the significance of that change, and what network features i.e., graph measures would be most influenced.

To answer this question, GTA was applied to each matrix, both NC and SR conditions, in every frequency band for each subject individually. This resulted in 22 sets of indices in 4 frequency bands for each subject.

5.3. Plotting Graph Measures

Certain global graph measures were chosen to track the brain network alteration: the graph density; global efficiency to assess the brain network integration; clustering coefficient and modularity to assess the network segregation and localized information processing

efficiency: average degree centrality of the network to assess the balanced state of the brain between organization and randomness i.e., heightened clustering and global efficiency, respectively; and assortativity to assess the network's ability to maintain structural integrity against destructions. Each graph index was averaged for all subjects pre- and post- SR and was plotted over time. A relatively high standard deviation was found in NC and SR indices at every timepoint. Individual subjects' indices spread out around the mean values that NC data frequently overlaps with SR. The following results are based on the trends observed in the averaged indices over the P300 ERP epoch duration from -100 to 1100 msec.

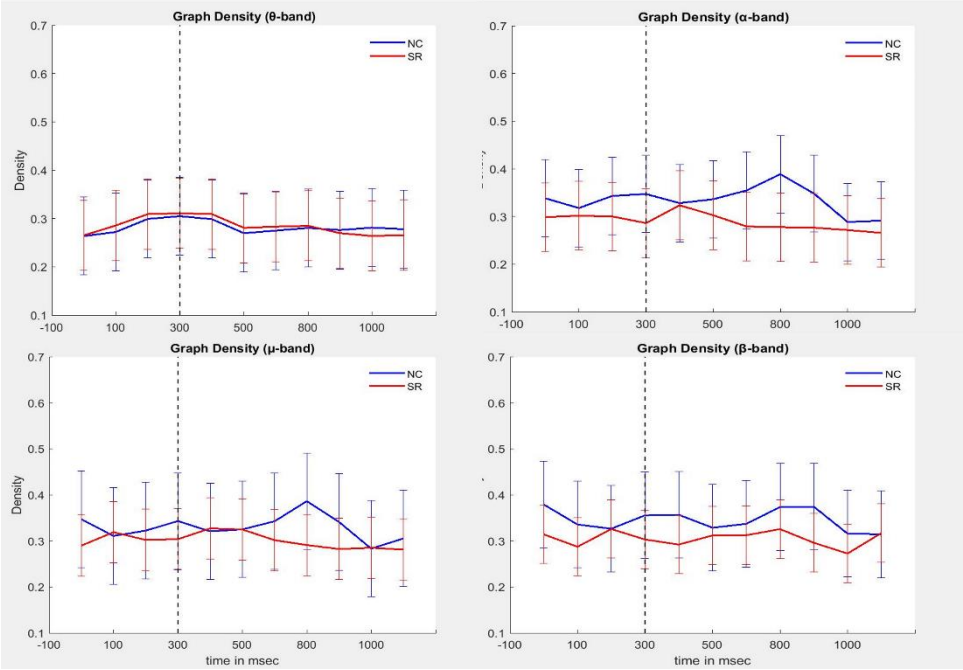

Figure 18: Graph Density of absolute-thresholded NC and SR networks plotted over time in every frequency band.

Figure 18 shows the difference in graph density after applying the absolute threshold to construct the matrices. θ- and μ- bands appear to exhibit the smallest difference between both states. In contrast, α- and β- bands seem to have the largest difference. SR graph density appears to be much lower than NC across the frequency bands, except for the θ- band. A slight increase in density of NC network occurs at 300 msec, which indicates generally higher connections between nodes in the brain as a cognitive response is triggered. Another peak can

be observed at 800 msec. This peak can also be found in subsequent figures of graph measures including the local average clustering coefficient, global efficiency and average degree centrality. In contrast the graph density of SR networks showed little change over time and slightly decreased in the α- and β- bands at 300 msec.

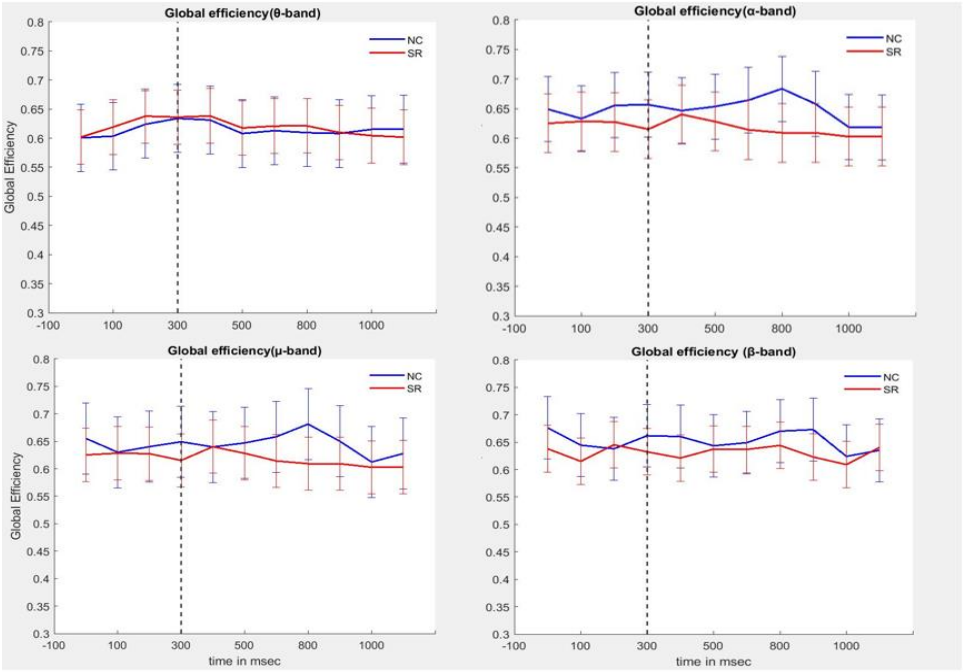

Figure 19: Global Efficiency index of NC and SR networks plotted over time in every frequency band.

Figure 19 demonstrates the global efficiency index, that is the inverse of the characteristic path length in each frequency band. The largest difference can be seen in the α-band, particularly at 300 msec and 800 msec. Since global efficiency is the inverse of the average pathlength of a network, the increase in global efficiency indicates better integration of the brain network with shorter path lengths between node facilitating higher efficiency of information processing. Global efficiency is generally higher in NC networks in all frequencies, except for the θ- band. In the α- band, the global efficiency is found to remain constant between 200 and 400 msec, whereas a small decrease is found in SR networks, specifically in the α- band, with an increase occurring after 300 msec.

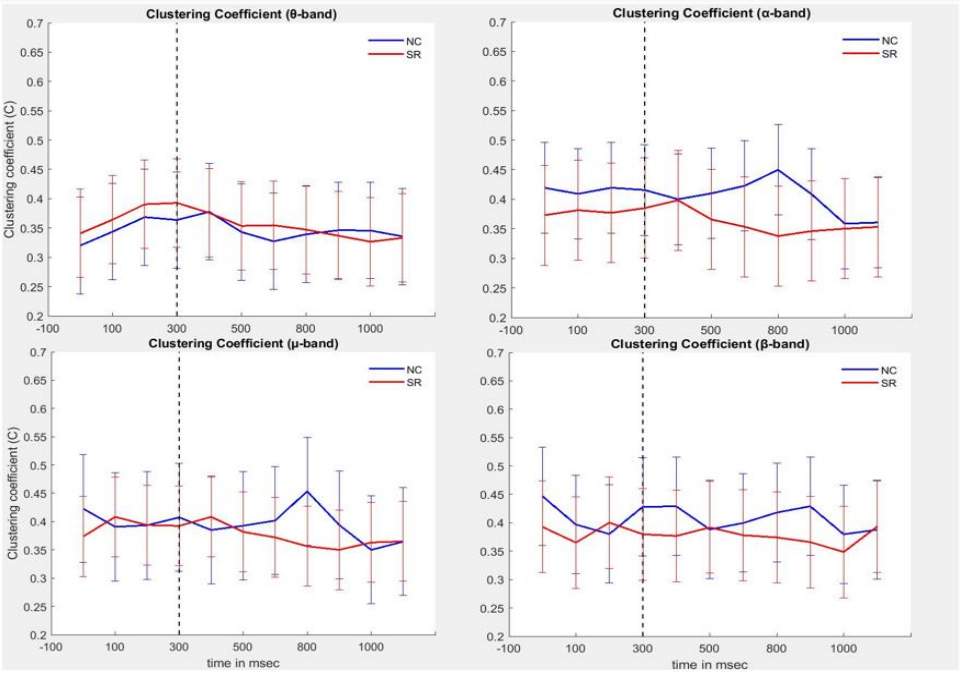

Figure 20: Clustering coefficient index plotted over time for NC and SR networks in every frequency band.

Figure 20 demonstrates the average local clustering coefficient or the average intra-connections within a cluster. A small difference is found in average NC and SR clustering coefficients with multiple points of intersection in most frequency bands. The α- band seems to have the largest difference between NC and SR plots at most timepoints. Clustering coefficient plateaus in SR and considerably drops after 400 msec, while it slightly increases in NC at 300 msec and 800 msec in α- and β- frequency bands.

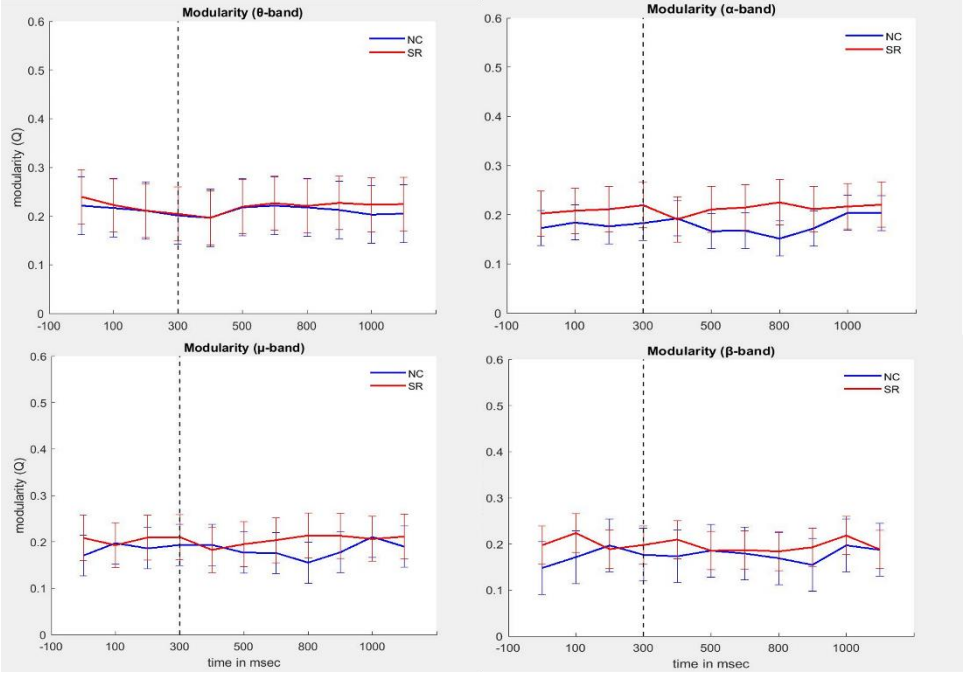

Figure 21: Modularity index plotted over time for NC and SR networks in every frequency band.

Figure 21 presents the change of network modularity. Unlike the previously described measures, average SR modularity is generally higher compared to NC. To reiterate, modularity is a measure of the degree to which a network can be divided into separate communities of nodes i.e., modules. Highly modular networks tend to have dense connections between the nodes in the same module, but weak connections i.e., longer path lengths between nodes in different modules. Particularly at 300 msec in the α- band that exhibits the largest difference between both conditions over time.

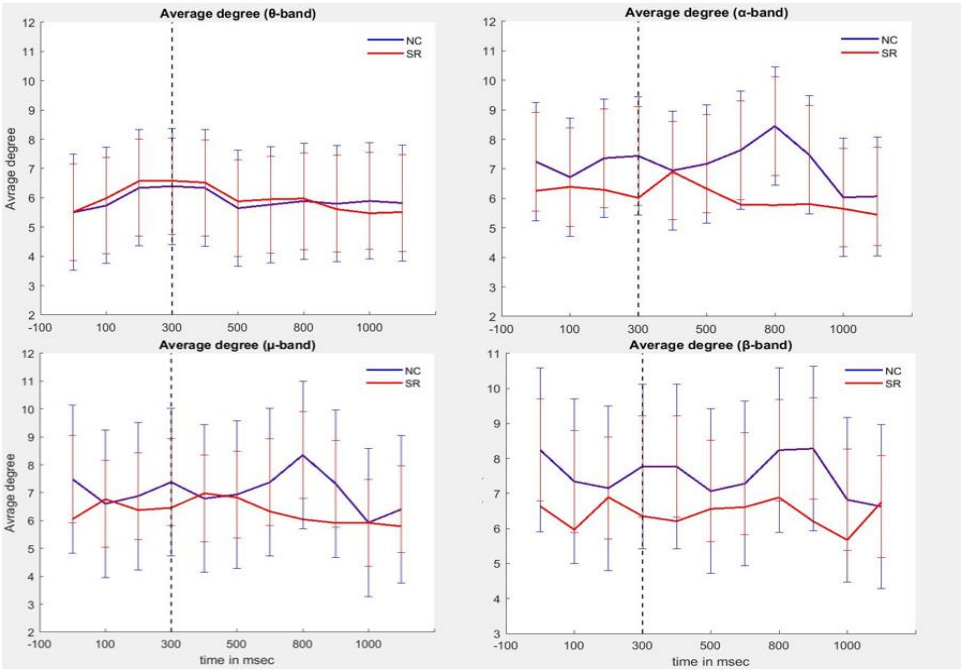

Figure 22: Average Degree Centrality index plotted over time for NC and SR networks in every frequency band.

The average degree of a network describes the average level of connectivity of individual nodes in a cluster. An increase in NC network average degree can be observed at 300 msec in α-, μ- and β- bands, Average degree of SR networks slightly increases after 300 msec in the α- and μ- band. The average degree centrality changing pattern over time is very similar to that found in the graph density, global efficiency and clustering coefficient, only scaled differently. This could suggest a linear relationship between those measures.

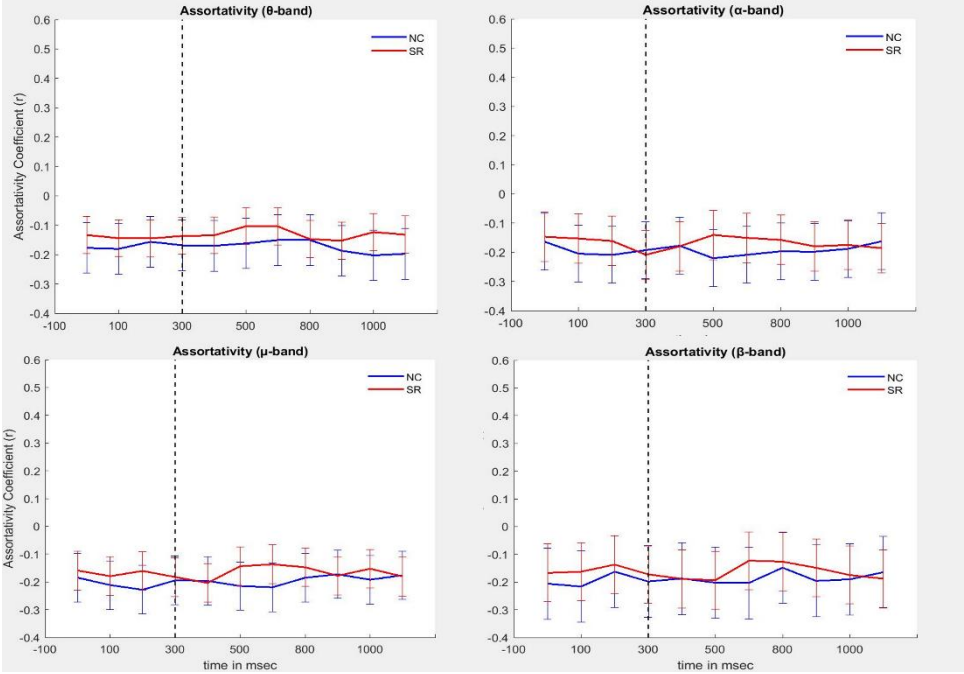

Figure 23: Assortativity index plotted over time for NC and SR networks in every frequency band.

Figure 23 represents the assortativity measure in NC and SR over time. To reiterate, assortativity is a measure that describes the extent to which nodes of similar degrees are more densely connected in a graph. Positive assortativity, closer to +1 indicates that similar nodes are connected to a large extent forming an assortative network, while negative assortativity, closer to -1 indicates a rather disassortative network where nodes of similar degree centrality aren't necessarily connected. In this data set, SR exhibits generally higher assortativity average, and a small difference between NC and SR average network assortativity was observed across the frequency bands. Network assortativity of both groups fall within the range of (-0.1 to -0.2) meaning that the average networks of both groups tend to be neutrally assortative.

5.4. Statistical Results

In the present study, the relationship between baseline brain network graph indices and changes (post- SR intervention minus pre-intervention) was examined. First, graph measures were quantified from connectivity matrices every 10 msec post-stimulus (between 0 and 1000msec) to be plotted over time. Each graph measure was averaged separately for all subjects' baseline, normal control (NC) and SR data (n=11). Paired t-test was performed for each measure in every frequency band. Graph indices derived from absolute-thresholded data were significantly influenced by SR in all frequency bands as shown in table 3.

All graph measures were strongly influenced by SR intervention in most of the frequency bands. The most significant changes in network features were mainly found in the α- band ($p < 0.001$) in 4 out of 6 graph measures and ($p<0.05$) in the remaining 2 indices; clustering coefficient and assortativity. Those two measures, however, were not significantly affected in μ- band. Furthermore, all graph measures were influenced in β- band ($p < 0.05$). In contrast, the difference in graph measures in the θ- band were of least significance. Particularly, the density was expected to be highly influenced in both conditions across all frequency bands after applying the absolute threshold to connectivity matrices. Nonetheless, the density wasn't strongly influenced in the θ-band.

Table 3: Paired t-test statistical results for each graph index in all frequency bands.

Graph Index	**Θ-Band 4 – 8 Hz**		**α- Band 8 – 13 Hz**		**μ-Band 10 – 12 Hz**		**β-Band 13 – 30 Hz**	
	p-value	**StD**	**p-value**	**StD**	**p-value**	**StD**	**p-value**	**StD**
Density	**p = 0.406**	0.0102	**p < 0.001**	0.0318	**p = 0.015**	0.0330	**p < 0.001**	0.0267
Global Efficiency	**p = 0.165**	0.0094	**p < 0.001**	0.0213	**p = 0.022**	0.0213	**p = 0.004**	0.0186
Clustering Coefficient	**p = 0.002**	0.0146	**p = 0.002**	0.0288	**p = 0.064**	0.0320	**p = 0.005**	0.0246
Modularity	**p = 0.007**	0.0081	**p < 0.001**	0.0200	**p = 0.009**	0.0209	**p = 0.007**	0.0206
Avg Degree Centrality	**p = 0.583**	0.2384	**p < 0.001**	0.7755	**p = 0.012**	0.7866	**p < 0.001**	0.6641
Assortativity	**p < 0.001**	0.0221	**p = 0.025**	0.0325	**p =0.077**	0.0319	**p = 0.012**	0.0281

Chapter 6. Discussion

The use of Graph Theoretic Analysis (GTA) on functional connectivity results provides a holistic perspective on brain network alterations. Functional Connectivity (FC) results rely on comparing one pair of channels at a time to assess the phase synchronization between them. GTA also characterizes different topographical features in the brain network which demonstrate the underlying neuronal interactions.

wPLI Measure: Assessing phase synchronization using the weighted phase-lag index (wPLI) has been used in multiple studies involving control and patient groups with cognitive decline conditions such as mild cognitive impairment (MCI) and Alzheimer's disease (AD). A decrease in wPLI was observed in patient groups compared to healthy controls. wPLI is an effective measure for assessing functional connectivity as it eliminates volume conduction effect, where multiple electrodes pick up on the same source of signal, giving a false indication of connectivity between the channels, this measure does not completely eliminate instantaneous synchronization, it rather gives smaller weights to phase differences close to 0 or π. This minimizes the effect of volume conduction while keeping the maximum amount of data, which adds to the robustness of the connectivity results.

Sleep Restriction Brain Model: The effect of sleep deprivation can be considered a small-scale model of an MCI network, as similar cognitive decline symptoms are observed in individuals suffering from insomnia and other sleep deficiency conditions. On a physiological level, amyloid β- (Aβ) is a protein naturally produced by the brain as a result of regular neuronal activity. The clearance of Aβ, along with other metabolic byproducts from the brain essentially occurs during sleep. Sleep deprivation was found to be associated with an increase in Aβ protein accumulation in the brain, a major biomarker of Alzheimer's disease, only with smaller level of severity. Unlike resting EEG, a cognitive, visual oddball paradigm test allowed investigating the effect of sleep restriction (SR) on cognitive functions, particularly

by triggering and extracting the P300 ERPs to analyze the brain connectivity over a certain cognitive domain: memory and attention.

Matrices Construction: Constructing adjacency matrices containing connectivity results facilitates the evaluation of the brain network features and allows for the comparison between different cognitive states and pathological conditions. An absolute threshold of 0.5 was applied to all constructed adjacency matrices, since the threshold value of 0.5 was commonly chosen among a range of thresholds in multiple brain research studies that adopt graph-based analysis. The thresholding step eliminated weaker connections in NC and SR networks. This explains why many synchronization values represented in SR matrices are set to 0. This is in fact due to the subthreshold connections between the neural elements (channels) that were mostly canceled out. Absolute-thresholded matrices exhibited clear differences between the α- band and other frequency bands in the control conditions, as well as between control and SR matrices. Control and SR topologies demonstrated differences in weights and density of edges connecting the graph nodes. SR had significantly smaller number of edges compared to controls, and dimmer colors in matrices indicating low synchronization levels. It's important to note that the mostly blue pixels in SR matrices are subthreshold synchronization values that were zeroed out due to the applied threshold. This technique could clearly emphasize the significance of brain connections in both conditions.

GTA Results: After applying GTA, network level alterations were quantified. GTA is an effective tool to detect temporary changes in the brain network due to changes in the cognitive state and can be used as a tool to diagnose or predict cognitive impairment conditions and early onset of Alzheimer’s.

Statistical Significance: In this study, the influence of SR-induced mental fatigue on the brain was found to be most significant in the α- band, where the largest changes in most

graph indices ($p < 0.001$) as well as the assortativity and clustering coefficient ($p < 0.05$) were observed. α- waves are produced by the brain and are associated with relaxed state of consciousness, α- band is also associated with memory, focus and attention. Matrices in the α- band demonstrated the most remarkable differences between both conditions across the subjects. Similar to α- band, β- band is associated with sensory processing including, attention, working memory and audiovisual integration [37], although it's mostly produced during an active state of consciousness unlike the α- band. All measures were found to be significantly impacted in the β- band ($p < 0.05$). In contrast, the μ- band is typically associated with motor response. The range of frequencies in the μ- band are close to the upper range of the α- band, which can justify the presence of a significant difference in synchronization levels in this band compared to the corresponding SR matrix at the same range of frequencies. The significant influence in the μ- band could also be associated with the repetitive right and left finger movement instructed during the test to sustain the subject's focus on the presented stimuli.

Network Density: The graph density of SR networks showed little change over time and slightly decreased in the α- and β- bands at 300 msec. This could also be due to some connections' weights dropping below the threshold value during the face recognition task in the mental fatigue state. High clustering coefficient, global efficiency and average degree could be directly related to the high connection density found in NC networks.

Segregation and Integration: Global efficiency and clustering coefficient were found to be higher in average NC condition. Both measures in NC plots increased at 300 msec where the P300 was expected. The differences occur in SR plots where global efficiency decreases at 300 msec, while clustering coefficient in SR remained almost constant. It might be easier to impact the network global efficiency while the clustering coefficient show better stability or little change in different cognitive states. A smaller SR

average clustering coefficient was expected, but the opposite was expected to be found in global efficiency according to studies that examines brain networks of cognitive decline conditions, an increase in SR global efficiency was expected due to the brain network's higher tendency to randomness as a result of mental fatigue. This could be attributed to a different mechanism of the brain in response to stimuli in minor mental fatigue compared to more severe pathological conditions such as mild cognitive impairment or Alzheimer's disease, especially that the chosen age group for the experiment were young adults (18-30 years of age), where the brain might exhibit certain adaptation mechanism to mildly stressful conditions, particularly following temporary sleep loss. Quantifying both measures over different brain regions i.e., subnetworks might give a better indication of the balance between segregation and integration in the overall brain small-world network model.

Network Centrality: Multiple centrality indices can be used to describe the small-world-ness of a network. The average degree centrality changing pattern over time was very similar to that found in clustering coefficient and global efficiency. The similarity between average degree and density measures seems intuitive, as more connections included to represent the network will increase the number of connections between one node and every other node. However, the similarity with global efficiency and clustering coefficient changing patterns might also be associated with the brain mechanism of preserving the small-world network characteristics. The human brain network is typically organized as a small-world network, essentially with both high clustering coefficient and shorter path lengths (higher global efficiency). Varying results in current research were found in regard to expected changes in the brain network indicating by cognitive decline conditions. Some studies indicate that regular network organizations are more likely to be exhibited in such conditions, while other studies would argue that randomness is expected. It is possible that the network organization of the brain model of one condition varies depending on the cognitive domain

being investigated. Moreover, A lower density is associated with lower wPLI values in SR network, which will decrease the clustering coefficient and global efficiency, irrespective of alteration in the structure of the network [83]. Based on the insight gained from the present analysis conducted with NC-SR data set, it could be presumed that the imbalance of small world-ness is an indication of cognitive decline. This loss of balance can be indicated by a decrease in global efficiency, local efficiency or the decrease in both features. Generally, the transition of a small-world network to randomness occurs as local connections rewire to connect distant nodes in a way that causes rapid reduction in path lengths with a relatively slow decrease in the local clustering coefficient [93]. This might suggest that clustering coefficient can be controlled to balance out the rapidly changing pathlength to some extent before the latter decreases rapidly, and unproportionally. This can better explain why average degree centrality appears to be linearly related to global efficiency and clustering coefficient in a minor mental fatigue state.

800 msec Peak: A remarkable peak appeared at 800 msec was found in NC plots in multiple measures including, but not limited to global efficiency and clustering coefficient. This might be attributed to the occurrence of late positive potential, another ERP elicited at visual cortical areas that is involved with emotional regulation. These ERPs might have been elicited as memories of the presented familiar face were prompted.

Modularity: Modularity was found to be generally higher in SR networks, indicating densely packed connections within the same cluster and longer path lengths (weaker connections) between distant clusters. Although better segregation was expected to be found in NC, Modular segregation is related to reduced capacity of global information exchange[94]. Global efficiency was found higher in NC networks, which indicates strong connections between distant nodes and between-modules connections. This justifies the increased modularity in SR networks since their global efficiency is much lower with longer

path lengths between distant nodes. Average SR modularity slightly drops in after the 300 msec timepoint, which might indicate increased integration of the brain network to process the presented stimuli (familiar faces).

Assortativity: The neutral assortativity, also referred to as weak disassortativity, in both conditions could be attributed to the presence of several nodes are significantly higher than other nodes in the network, these nodes connect to other prevalent lower degree nodes, which would affect the robustness of the network. Assortativity might serve as a better indicator of robustness based on network organization if applied to separate parts of the brain rather than the entire network. However, it has been previously pointed out that positive assortativity is more likely to be exhibited when examining structural connectivity rather than functional connectivity to ensure network robustness, disassortative functional network could be the mechanism of the brain to limit the extent of exchanged neuronal information across the network to control the propagation of abnormal brain activity such as epileptic seizures[78]. However, examining the differences between left and right hemisphere assortativity might give a better description of the brain network assortativity in sleep disorder models studies. The brain network can undergo an increase of a certain network feature at one brain region but not the other, depending on the task or stimulus being triggered.

Absolute and Proportional Threshold: Before reporting the analysis results of absolute-thresholded data, a proportional threshold of 0.5 (50%) was applied to the set of matrices and the analysis was repeated for comparison. To reiterate, the proportional threshold maintains a constant graph density across networks of both conditions. Although the proportional average degree centrality was found to differ significantly across the frequency bands, other measures were similar to the current absolute-thresholded networks results with considerably smaller differences between NC and SR conditions.

Furthermore, A very subtle difference in global efficiency was observed across most frequency bands, where the global efficiency of NC and SR plots were constant and almost overlapping over time. The clustering coefficient was higher in SR than in NC. The inconsistency in results could be attributed to the presence of weak, unreliable connections that were included in the proportional-thresholded data to preserve a constant graph density, which distorted the results.

Limitations: There are still limitations that need further consideration in this study. This study considered only global characteristics of brain networks and their influence on network connectivity. Further studies should investigate spatial alterations of brain networks by analyzing and comparing the values of graph-based indices in multiple brain regions over time or use. Utilizing an EEG cap of 64 channels or more can also provide a better understanding of the brain dynamics and features with higher resolution. Furthermore, a larger sample size is needed to give more meaningful statistical results and lower the standard deviation. This will also give a definite pattern of change in each measure over time to better explain the brain dynamics in response to stimuli requiring focus and attention. Similarly, more studies are needed to describe the alterations in connectivity patterns over time in sleep disorders to understand the underlying mechanisms of information processing through the brain network and its effect on performance and cognition in sleep-related conditions. Finally, more studies on different threshold types and values are necessary to identify consensus by which the optimal representation of data is achieved depending on the brain condition and types of studies i.e., case-control, between-subjects, and within-subjects experiments.

Chapter 7. Conclusion

Functional connectivity and graph theory-based analyses can be particularly useful to detect networks level changes in the development of cognitive decline conditions and sleep disorders. Graph theoretic analysis provides a full topological representation of the brain network in graphs, which provides more information about the cognitive state at a certain time point, rather than comparing functional connectivity results between channel pairs. Moreover, implementing this approach facilitates monitoring cognitive impairment progression and detecting the early onset of neurodegenerative disorders. When using a visual oddball task with familiar face images, subjects showed a significant change in response to the stimuli in SR condition compared to control networks. Lower local connections and longer path lengths are found as a result of mental fatigue, which impacts information processing efficiency. This was apparent even when the induced condition was far simpler than total and partial sleep deprivation The alteration in network features was most significant in the α- frequency range, reflecting the impact of sleep loss on attention and memory processing. Graph theoretic analysis provides instrumental information on subtle network-level changes of the brain which manifest themselves as network differences where lower local and global network efficiency in response to stimuli, most possibly related to diminished memory processing.

References

[1] S. Sadeghmousavi, M. Eskian, F. Rahmani, and N. Rezaei, “The effect of insomnia on development of Alzheimer’s disease,” *J. Neuroinflammation*, vol. 17, no. 1, p. 289, Dec. 2020, doi: 10.1186/s12974-020-01960-9.

[2] “Dementia.” https://www.who.int/news-room/fact-sheets/detail/dementia (accessed Feb. 03, 2022).

[3] J. C. Morris *et al.*, “Mild cognitive impairment represents early-stage Alzheimer disease,” *Arch. Neurol.*, vol. 58, no. 3, pp. 397–405, Mar. 2001, doi: 10.1001/archneur.58.3.397.

[4] S. Palmqvist *et al.*, “Earliest accumulation of β-amyloid occurs within the default-mode network and concurrently affects brain connectivity,” *Nat. Commun.*, vol. 8, no. 1, Art. no. 1, Oct. 2017, doi: 10.1038/s41467-017-01150-x.

[5] X. Zhang, Z. Fu, L. Meng, M. He, and Z. Zhang, “The Early Events That Initiate β-Amyloid Aggregation in Alzheimer’s Disease,” *Front. Aging Neurosci.*, vol. 10, p. 359, Nov. 2018, doi: 10.3389/fnagi.2018.00359.

[6] B. Rasch and J. Born, “About Sleep’s Role in Memory,” *Physiol. Rev.*, vol. 93, no. 2, pp. 681–766, Apr. 2013, doi: 10.1152/physrev.00032.2012.

[7] S. Cordone, L. Annarumma, P. M. Rossini, and L. De Gennaro, “Sleep and β-Amyloid Deposition in Alzheimer Disease: Insights on Mechanisms and Possible Innovative Treatments,” *Front. Pharmacol.*, vol. 10, 2019, Accessed: Feb. 04, 2022. [Online]. Available: https://www.frontiersin.org/article/10.3389/fphar.2019.00695

[8] A. M. V. Wennberg, M. N. Wu, P. B. Rosenberg, and A. P. Spira, “Sleep Disturbance, Cognitive Decline, and Dementia: A Review,” *Semin. Neurol.*, vol. 37, no. 4, pp. 395–406, Aug. 2017, doi: 10.1055/s-0037-1604351.

[9] E. Shokri-Kojori *et al.*, “β-Amyloid accumulation in the human brain after one night of sleep deprivation,” *Proc. Natl. Acad. Sci. U. S. A.*, vol. 115, no. 17, pp. 4483–4488, Apr. 2018, doi: 10.1073/pnas.1721694115.

[10] “Lack of sleep in middle age may increase dementia risk,” *National Institutes of Health (NIH)*, Apr. 27, 2021. https://www.nih.gov/news-events/nih-research-matters/lack-sleep-middle-age-may-increase-dementia-risk (accessed Feb. 23, 2022).

[11] P. Alhola and P. Polo-Kantola, “Sleep deprivation: Impact on cognitive performance,” *Neuropsychiatr. Dis. Treat.*, vol. 3, no. 5, pp. 553–567, Oct. 2007.

[12] F. D. V. Fallani, J. Richiardi, M. Chavez, and S. Achard, “Graph analysis of functional brain networks: practical issues in translational neuroscience,” *Philos. Trans. R. Soc. B Biol. Sci.*, vol. 369, no. 1653, p. 20130521, Oct. 2014, doi: 10.1098/rstb.2013.0521.

[13] J. M. Dzierzewski, N. Dautovich, and S. Ravyts, “Sleep and Cognition in the Older Adult,” *Sleep Med. Clin.*, vol. 13, no. 1, pp. 93–106, Mar. 2018, doi: 10.1016/j.jsmc.2017.09.009.

[14] “APA Dictionary of Psychology.” https://dictionary.apa.org/ (accessed Feb. 15, 2022).

[15] D. D. Correa, M. Kryza-Lacombe, R. E. Baser, K. Beal, and L. M. DeAngelis, “COGNITIVE EFFECTS OF DONEPEZIL THERAPY IN PATIENTS WITH BRAIN TUMORS: A PILOT STUDY,” *J. Neurooncol.*, vol. 127, no. 2, pp. 313–319, Apr. 2016, doi: 10.1007/s11060-015-2035-3.

[16] M. S. D'Souza, "Brain and Cognition for Addiction Medicine: From Prevention to Recovery Neural Substrates for Treatment of Psychostimulant-Induced Cognitive Deficits," *Front. Psychiatry*, vol. 10, 2019, Accessed: Feb. 15, 2022. [Online]. Available: https://www.frontiersin.org/article/10.3389/fpsyt.2019.00509

[17] F. Bernardin, A. Maheut-Bosser, and F. Paille, "Cognitive Impairments in Alcohol-Dependent Subjects," *Front. Psychiatry*, vol. 5, 2014, Accessed: Feb. 15, 2022. [Online]. Available: https://www.frontiersin.org/article/10.3389/fpsyt.2014.00078

[18] H. M. Brothers, M. L. Gosztyla, and S. R. Robinson, "The Physiological Roles of Amyloid-β Peptide Hint at New Ways to Treat Alzheimer's Disease," *Front. Aging Neurosci.*, vol. 10, p. 118, Apr. 2018, doi: 10.3389/fnagi.2018.00118.

[19] Z. Arvanitakis, R. C. Shah, and D. A. Bennett, "Diagnosis and Management of Dementia: A Review," *JAMA*, vol. 322, no. 16, pp. 1589–1599, Oct. 2019, doi: 10.1001/jama.2019.4782.

[20] C. G. Fernandez, M. E. Hamby, M. L. McReynolds, and W. J. Ray, "The Role of APOE4 in Disrupting the Homeostatic Functions of Astrocytes and Microglia in Aging and Alzheimer's Disease," *Front. Aging Neurosci.*, vol. 11, 2019, Accessed: Feb. 16, 2022. [Online]. Available: https://www.frontiersin.org/article/10.3389/fnagi.2019.00014

[21] C. A. Gold and A. E. Budson, "Memory loss in Alzheimer's disease: implications for development of therapeutics," *Expert Rev. Neurother.*, vol. 8, no. 12, pp. 1879–1891, Dec. 2008, doi: 10.1586/14737175.8.12.1879.

[22] J. Khaw, P. Subramaniam, N. A. Abd Aziz, A. Ali Raymond, W. A. Wan Zaidi, and S. E. Ghazali, "Current Update on the Clinical Utility of MMSE and MoCA for Stroke Patients in Asia: A Systematic Review," *Int. J. Environ. Res. Public. Health*, vol. 18, no. 17, p. 8962, Aug. 2021, doi: 10.3390/ijerph18178962.

[23] A. Kaur, S. D. Edland, and G. M. Peavy, “The MoCA Memory Index Score: An Efficient Alternative to Paragraph Recall for the Detection Of Amnestic Mild Cognitive Impairment,” *Alzheimer Dis. Assoc. Disord.*, vol. 32, no. 2, pp. 120–124, 2018, doi: 10.1097/WAD.0000000000000240.

[24] Y. Kaya, O. E. Aki, U. A. Can, E. Derle, S. Kibaroğlu, and A. Barak, “Validation of Montreal Cognitive Assessment and Discriminant Power of Montreal Cognitive Assessment Subtests in Patients With Mild Cognitive Impairment and Alzheimer Dementia in Turkish Population,” *J. Geriatr. Psychiatry Neurol.*, vol. 27, no. 2, pp. 103–109, Jun. 2014, doi: 10.1177/0891988714522701.

[25] S. Hoops *et al.*, “Validity of the MoCA and MMSE in the detection of MCI and dementia in Parkinson disease,” *Neurology*, vol. 73, no. 21, pp. 1738–1745, Nov. 2009, doi: 10.1212/WNL.0b013e3181c34b47.

[26] R. W. Paterson *et al.*, “Cerebrospinal fluid in the differential diagnosis of Alzheimer’s disease: clinical utility of an extended panel of biomarkers in a specialist cognitive clinic,” *Alzheimers Res. Ther.*, vol. 10, no. 1, p. 32, Mar. 2018, doi: 10.1186/s13195-018-0361-3.

[27] M. Ewers *et al.*, “CSF biomarkers for the differential diagnosis of Alzheimer’s disease: A large-scale international multicenter study,” *Alzheimers Dement. J. Alzheimers Assoc.*, vol. 11, no. 11, pp. 1306–1315, Nov. 2015, doi: 10.1016/j.jalz.2014.12.006.

[28] C. Marcus, E. Mena, and R. M. Subramaniam, “Brain PET in the Diagnosis of Alzheimer’s Disease,” *Clin. Nucl. Med.*, vol. 39, no. 10, pp. e413–e426, Oct. 2014, doi: 10.1097/RLU.0000000000000547.

[29] M. A. Oghabian, S. A. H. Batouli, M. Norouzian, M. Ziaei, and H. Sikaroodi, “Using functional Magnetic Resonance Imaging to differentiate between healthy aging subjects, Mild Cognitive Impairment, and Alzheimer’s patients,” *J. Res. Med. Sci. Off. J. Isfahan Univ. Med. Sci.*, vol. 15, no. 2, pp. 84–93, 2010.

[30] J. Parvizi and S. Kastner, “Human Intracranial EEG: Promises and Limitations,” *Nat. Neurosci.*, vol. 21, no. 4, pp. 474–483, Apr. 2018, doi: 10.1038/s41593-018-0108-2.

[31] G. Buzsáki, C. A. Anastassiou, and C. Koch, “The origin of extracellular fields and currents — EEG, ECoG, LFP and spikes,” *Nat. Rev. Neurosci.*, vol. 13, no. 6, pp. 407–420, May 2012, doi: 10.1038/nrn3241.

[32] Z. R. Cross, M. J. Kohler, M. Schlesewsky, M. G. Gaskell, and I. Bornkessel-Schlesewsky, “Sleep-Dependent Memory Consolidation and Incremental Sentence Comprehension: Computational Dependencies during Language Learning as Revealed by Neuronal Oscillations,” *Front. Hum. Neurosci.*, vol. 12, 2018, Accessed: Feb. 23, 2022. [Online]. Available: https://www.frontiersin.org/article/10.3389/fnhum.2018.00018

[33] A. K. Bourisly and A. Shuaib, “Neurophysiological Effects of Aging: A P200 ERP Study,” *Transl. Neurosci.*, vol. 9, pp. 61–66, Jun. 2018, doi: 10.1515/tnsci-2018-0011.

[34] H. Benveniste, X. Liu, S. Koundal, S. Sanggaard, H. Lee, and J. Wardlaw, “The Glymphatic System and Waste Clearance with Brain Aging: A Review,” *Gerontology*, vol. 65, no. 2, pp. 106–119, 2019, doi: 10.1159/000490349.

[35] G. M. Ashraf *et al.*, “Protein misfolding and aggregation in Alzheimer’s disease and Type 2 Diabetes Mellitus,” *CNS Neurol. Disord. Drug Targets*, vol. 13, no. 7, pp. 1280–1293, 2014.

[36] Z. Peng, C. Dai, Y. Ba, L. Zhang, Y. Shao, and J. Tian, “Effect of Sleep Deprivation on the Working Memory-Related N2-P3 Components of the Event-Related Potential Waveform,” *Front. Neurosci.*, vol. 14, 2020, Accessed: Feb. 25, 2022. [Online]. Available: https://www.frontiersin.org/article/10.3389/fnins.2020.00469

[37] L. Wang *et al.*, “Beta-Band Functional Connectivity Influences Audiovisual Integration in Older Age: An EEG Study,” *Front. Aging Neurosci.*, vol. 9, 2017, Accessed: Mar. 31, 2023. [Online]. Available: https://www.frontiersin.org/articles/10.3389/fnagi.2017.00239

[38] G. Buzsaki, C. A. Anastassiou, and C. Koch, “The origin of extracellular fields and currents--EEG, ECoG, LFP and spikes,” *Nat. Rev. Neurosci.*, vol. 13, no. 6, pp. 407–421, Jun. 2012, doi: 10.1038/nrn3241.

[39] L. Dong *et al.*, “A Comparative Study of Different EEG Reference Choices for Event-Related Potentials Extracted by Independent Component Analysis,” *Front. Neurosci.*, vol. 13, p. 1068, Oct. 2019, doi: 10.3389/fnins.2019.01068.

[40] T. Picton and D. Stuss, “The Component Structure of the Human Event-Related Potentials,” *Prog. Brain Res.*, vol. 54, pp. 17–48, Feb. 1980, doi: 10.1016/S0079-6123(08)61604-0.

[41] G. F. Woodman, “A Brief Introduction to the Use of Event-Related Potentials (ERPs) in Studies of Perception and Attention,” *Atten. Percept. Psychophys.*, vol. 72, no. 8, p. 10.3758/APP.72.8.2031, Nov. 2010, doi: 10.3758/APP.72.8.2031.

[42] D. Amodio, B. Bartholow, and T. Ito, “Tracking the dynamics of the social brain: ERP approaches for Social Cognitive & Affective Neuroscience.,” *Soc. Cogn. Affect. Neurosci.*, vol. 9, Dec. 2013, doi: 10.1093/scan/nst177.

[43] "An Introduction to the Event-Related Potential Technique.pdf." Accessed: Sep. 27, 2021. [Online]. Available: https://www.ncbs.res.in/sitefiles/gb2012/An%20Introduction%20to%20the%20Event-Related%20Potential%20Technique.pdf

[44] M. Mück, K. Ohmann, S. Dummel, A. Mattes, U. Thesing, and J. Stahl, "Face Perception and Narcissism: Variations of Event-Related Potential Components (P1 & N170) with Admiration and Rivalry," *Cogn. Affect. Behav. Neurosci.*, vol. 20, no. 5, pp. 1041–1055, Oct. 2020, doi: http://dx.doi.org/10.3758/s13415-020-00818-0.

[45] S. H. Patel and P. N. Azzam, "Characterization of N200 and P300: Selected Studies of the Event-Related Potential," *Int. J. Med. Sci.*, vol. 2, no. 4, pp. 147–154, Oct. 2005.

[46] M. Lijffijt *et al.*, "P50, N100, and P200 sensory gating: Relationships with behavioral inhibition, attention, and working memory," *Psychophysiology*, vol. 46, no. 5, p. 1059, Sep. 2009, doi: 10.1111/j.1469-8986.2009.00845.x.

[47] J. P. Hamm, B. W. Johnson, and I. J. Kirk, "Comparison of the N300 and N400 ERPs to picture stimuli in congruent and incongruent contexts," *Clin. Neurophysiol.*, vol. 113, no. 8, pp. 1339–1350.

[48] B. Blankertz, S. Lemm, M. Treder, S. Haufe, and K.-R. Müller, "Single-trial analysis and classification of ERP components -- A tutorial," *NeuroImage*, vol. 56, no. 2, pp. 814–825, May 2011, doi: http://dx.doi.org/10.1016/j.neuroimage.2010.06.048.

[49] "Response speed, contingent negative variation and P300 in Alzheimer's disease and MCI | Elsevier Enhanced Reader." https://reader.elsevier.com/reader/sd/pii/S0278262608003345?token=8F98C1B4F0C86615DCBFCF8CDF630F2DD0AA3A38FD933A8DB16BF33FC0AFF79B6363C8C1B77D23F0A9437F893449E143&originRegion=us-east-1&originCreation=20220220180859 (accessed Feb. 20, 2022).

[50] S. Jiang *et al.*, “Using event-related potential P300 as an electrophysiological marker for differential diagnosis and to predict the progression of mild cognitive impairment: a meta-analysis,” *Neurol. Sci.*, vol. 36, no. 7, pp. 1105–1112, Jul. 2015, doi: 10.1007/s10072-015-2099-z.

[51] C. D. Papadaniil, V. E. Kosmidou, A. Tsolaki, M. Tsolaki, I. (Yiannis) Kompatsiaris, and L. J. Hadjileontiadis, “Cognitive MMN and P300 in mild cognitive impairment and Alzheimer’s disease: A high density EEG-3D vector field tomography approach,” *Brain Res.*, vol. 1648, pp. 425–433, Oct. 2016, doi: 10.1016/j.brainres.2016.07.043.

[52] R. N. Newsome, C. Pun, V. M. Smith, S. Ferber, and M. D. Barense, “Neural correlates of cognitive decline in older adults at-risk for developing MCI: evidence from the CDA and P300,” *Cogn. Neurosci.*, vol. 4, no. 3–4, pp. 152–162, 2013, doi: 10.1080/17588928.2013.853658.

[53] E. W. Lang, A. M. Tomé, I. R. Keck, J. M. Górriz-Sáez, and C. G. Puntonet, “Brain Connectivity Analysis: A Short Survey,” *Comput. Intell. Neurosci.*, vol. 2012, p. e412512, Oct. 2012, doi: 10.1155/2012/412512.

[54] M. Filippi, E. G. Spinelli, C. Cividini, and F. Agosta, “Resting State Dynamic Functional Connectivity in Neurodegenerative Conditions: A Review of Magnetic Resonance Imaging Findings,” *Front. Neurosci.*, vol. 13, p. 657, 2019, doi: 10.3389/fnins.2019.00657.

[55] Q. Chang *et al.*, “EEG-Based Brain Functional Connectivity in First-Episode Schizophrenia Patients, Ultra-High-Risk Individuals, and Healthy Controls During P50 Suppression,” *Front. Hum. Neurosci.*, vol. 13, p. 379, 2019, doi: 10.3389/fnhum.2019.00379.

[56] A. M. Bastos and J.-M. Schoffelen, “A Tutorial Review of Functional Connectivity Analysis Methods and Their Interpretational Pitfalls,” *Front. Syst. Neurosci.*, vol. 9, 2015, doi: 10.3389/fnsys.2015.00175.

[57] B. Horwitz, “The elusive concept of brain connectivity,” *NeuroImage*, vol. 19, no. 2, pp. 466–470, Jun. 2003, doi: 10.1016/S1053-8119(03)00112-5.

[58] H. E. Wang, C. G. Bénar, P. P. Quilichini, K. J. Friston, V. K. Jirsa, and C. Bernard, “A systematic framework for functional connectivity measures,” *Front. Neurosci.*, vol. 8, 2014, Accessed: Mar. 14, 2022. [Online]. Available: https://www.frontiersin.org/article/10.3389/fnins.2014.00405

[59] “Tracking brain states under general anesthesia by using global coherence analysis | PNAS.” https://www.pnas.org/content/108/21/8832 (accessed Oct. 23, 2021).

[60] C. A. Bosman *et al.*, “Attentional Stimulus Selection through Selective Synchronization between Monkey Visual Areas,” *Neuron*, vol. 75, no. 5, pp. 875–888, Sep. 2012, doi: 10.1016/j.neuron.2012.06.037.

[61] “Scopus preview - Scopus - Welcome to Scopus.” https://www.scopus.com/home.uri (accessed Oct. 23, 2021).

[62] W. R. Winter, P. L. Nunez, J. Ding, and R. Srinivasan, “Comparison of the effect of volume conduction on EEG coherence with the effect of field spread on MEG coherence,” *Stat. Med.*, vol. 26, no. 21, pp. 3946–3957, 2007, doi: 10.1002/sim.2978.

[63] A. J. Bell and T. J. Sejnowski, “The ‘independent components’ of natural scenes are edge filters,” *Vision Res.*, vol. 37, no. 23, pp. 3327–3338, Dec. 1997, doi: 10.1016/S0042-6989(97)00121-1.

[64] C. Bugli and P. Lambert, “Comparison between Principal Component Analysis and Independent Component Analysis in Electroencephalograms Modelling,” *Biom. J.*, vol. 49, no. 2, pp. 312–327, 2007, doi: 10.1002/bimj.200510285.

[65] T. Radüntz, J. Scouten, O. Hochmuth, and B. Meffert, “EEG artifact elimination by extraction of ICA-component features using image processing algorithms,” *J. Neurosci. Methods*, vol. 243, pp. 84–93, Mar. 2015, doi: 10.1016/j.jneumeth.2015.01.030.

[66] S. Aydore, D. Pantazis, and R. M. Leahy, “A Note on the Phase Locking Value and its Properties,” *NeuroImage*, vol. 74, pp. 231–244, Jul. 2013, doi: 10.1016/j.neuroimage.2013.02.008.

[67] M. X. Cohen, “Effects of time lag and frequency matching on phase-based connectivity,” *J. Neurosci. Methods*, vol. 250, pp. 137–146, Jul. 2015, doi: 10.1016/j.jneumeth.2014.09.005.

[68] C. J. Stam, G. Nolte, and A. Daffertshofer, “Phase lag index: assessment of functional connectivity from multi channel EEG and MEG with diminished bias from common sources,” *Hum. Brain Mapp.*, vol. 28, no. 11, pp. 1178–1193, Nov. 2007, doi: 10.1002/hbm.20346.

[69] M. Vinck, R. Oostenveld, M. van Wingerden, F. Battaglia, and C. M. A. Pennartz, “An improved index of phase-synchronization for electrophysiological data in the presence of volume-conduction, noise and sample-size bias,” *NeuroImage*, vol. 55, no. 4, pp. 1548–1565, Apr. 2011, doi: 10.1016/j.neuroimage.2011.01.055.

[70] F. V. Farahani, W. Karwowski, and N. R. Lighthall, “Application of Graph Theory for Identifying Connectivity Patterns in Human Brain Networks: A Systematic Review,” *Front. Neurosci.*, vol. 13, p. 585, 2019, doi: 10.3389/fnins.2019.00585.

[71] O. Sporns, “Graph theory methods: applications in brain networks,” *Dialogues Clin. Neurosci.*, vol. 20, no. 2, pp. 111–121, Jun. 2018.

[72] K. A. Garrison, D. Scheinost, E. S. Finn, X. Shen, and R. T. Constable, “The (in)stability of functional brain network measures across thresholds,” *NeuroImage*, vol. 118, pp. 651–661, Sep. 2015, doi: 10.1016/j.neuroimage.2015.05.046.

[73] M. P. van den Heuvel, S. C. de Lange, A. Zalesky, C. Seguin, B. T. T. Yeo, and R. Schmidt, “Proportional thresholding in resting-state fMRI functional connectivity networks and consequences for patient-control connectome studies: Issues and recommendations,” *NeuroImage*, vol. 152, pp. 437–449, May 2017, doi: 10.1016/j.neuroimage.2017.02.005.

[74] T. Adamovich, I. Zakharov, A. Tabueva, and S. Malykh, “The thresholding problem and variability in the EEG graph network parameters,” *Sci. Rep.*, vol. 12, no. 1, Art. no. 1, Nov. 2022, doi: 10.1038/s41598-022-22079-2.

[75] J. R. Cohen and M. D’Esposito, “The Segregation and Integration of Distinct Brain Networks and Their Relationship to Cognition,” *J. Neurosci.*, vol. 36, no. 48, pp. 12083–12094, Nov. 2016, doi: 10.1523/JNEUROSCI.2965-15.2016.

[76] K. A. Zweig, “Centrality Indices,” in *Network Analysis Literacy: A Practical Approach to the Analysis of Networks*, K. A. Zweig, Ed., in Lecture Notes in Social Networks. Vienna: Springer, 2016, pp. 243–276. doi: 10.1007/978-3-7091-0741-6_9.

[77] C. F. A. Negre *et al.*, “Eigenvector centrality for characterization of protein allosteric pathways,” *Proc. Natl. Acad. Sci. U. S. A.*, vol. 115, no. 52, pp. E12201–E12208, Dec. 2018, doi: 10.1073/pnas.1810452115.

[78] S. Lim, F. Radicchi, M. P. van den Heuvel, and O. Sporns, “Discordant attributes of structural and functional brain connectivity in a two-layer multiplex network,” *Sci. Rep.*, vol. 9, p. 2885, Feb. 2019, doi: 10.1038/s41598-019-39243-w.

[79] G. Mårtensson *et al.*, “Stability of graph theoretical measures in structural brain networks in Alzheimer’s disease,” *Sci. Rep.*, vol. 8, no. 1, Art. no. 1, Aug. 2018, doi: 10.1038/s41598-018-29927-0.

[80] “Frontiers | Diagnosis of Alzheimer’s Disease Using Brain Network | Neuroscience.” https://www.frontiersin.org/articles/10.3389/fnins.2021.605115/full (accessed Mar. 09, 2022).

[81] C. Ferguson and Alzheimer’s Disease Neuroimaging Initiative, “A network psychometric approach to neurocognition in early Alzheimer’s disease,” *Cortex J. Devoted Study Nerv. Syst. Behav.*, vol. 137, pp. 61–73, Apr. 2021, doi: 10.1016/j.cortex.2021.01.002.

[82] G. Tosi, C. Borsani, S. Castiglioni, R. Daini, M. Franceschi, and D. Romano, “Complexity in neuropsychological assessments of cognitive impairment: A network analysis approach,” *Cortex J. Devoted Study Nerv. Syst. Behav.*, vol. 124, pp. 85–96, Mar. 2020, doi: 10.1016/j.cortex.2019.11.004.

[83] C. J. Stam *et al.*, “Graph theoretical analysis of magnetoencephalographic functional connectivity in Alzheimer’s disease,” *Brain*, vol. 132, no. 1, pp. 213–224, Jan. 2009, doi: 10.1093/brain/awn262.

[84] L. M. Wright, M. De Marco, and A. Venneri, “A Graph Theory Approach to Clarifying Aging and Disease Related Changes in Cognitive Networks,” *Front. Aging Neurosci.*, vol. 13, p. 676618, Jul. 2021, doi: 10.3389/fnagi.2021.676618.

[85] F. V. Farahani *et al.*, “Effects of Chronic Sleep Restriction on the Brain Functional Network, as Revealed by Graph Theory,” *Front. Neurosci.*, vol. 13, 2019, Accessed: Mar. 29, 2022. [Online]. Available: https://www.frontiersin.org/article/10.3389/fnins.2019.01087

[86] S. I. Dimitriadis, M. Drakesmith, S. Bells, G. D. Parker, D. E. Linden, and D. K. Jones, “Improving the Reliability of Network Metrics in Structural Brain Networks by Integrating Different Network Weighting Strategies into a Single Graph,” *Front. Neurosci.*, vol. 11, 2017, Accessed: Mar. 09, 2022. [Online]. Available: https://www.frontiersin.org/article/10.3389/fnins.2017.00694

[87] A. Zalesky, A. Fornito, and E. Bullmore, “On the use of correlation as a measure of network connectivity,” *NeuroImage*, vol. 60, no. 4, pp. 2096–2106, May 2012, doi: 10.1016/j.neuroimage.2012.02.001.

[88] M. Basner, D. Mollicone, and D. F. Dinges, “Validity and Sensitivity of a Brief Psychomotor Vigilance Test (PVT-B) to Total and Partial Sleep Deprivation,” *Acta Astronaut.*, vol. 69, no. 11–12, pp. 949–959, Dec. 2011, doi: 10.1016/j.actaastro.2011.07.015.

[89] M. E. J. Newman, “Modularity and community structure in networks,” *Proc. Natl. Acad. Sci.*, vol. 103, no. 23, pp. 8577–8582, Jun. 2006, doi: 10.1073/pnas.0601602103.

[90] K.-K. Tang and A. Wagner, “Measuring globalization using weighted network indexes,” Apr. 2022.

[91] G. Thedchanamoorthy, M. Piraveenan, D. Kasthuriratna, and U. Senanayake, “Node Assortativity in Complex Networks: An Alternative Approach,” *Procedia Comput. Sci.*, vol. 29, pp. 2449–2461, Jan. 2014, doi: 10.1016/j.procs.2014.05.229.

[92] “SPSS Paired Samples T-Test - Quick Tutorial & Example.” https://www.spss-tutorials.com/spss-paired-samples-t-test/ (accessed Mar. 29, 2022).

[93] “Graph Theory,” Jan. 2014, doi: 10.7551/mitpress/9609.003.0038.

[94] G. L. Baum *et al.*, “Modular Segregation of Structural Brain Networks Supports the Development of Executive Function in Youth,” *Curr. Biol.*, vol. 27, no. 11, pp. 1561-1572.e8, Jun. 2017, doi: 10.1016/j.cub.2017.04.051.

Appendix A: IRB Approval

Antar, Marwa

From: UMCIRB
Sent: Friday, November 4, 2022 10:13 AM
To: Antar, Marwa
Subject: IRB: Study Correspondence Letter

EAST CAROLINA UNIVERSITY
University & Medical Center Institutional Review Board
4N-64 Brody Medical Sciences Building· Mail Stop 682
600 Moye Boulevard · Greenville, NC 27834
Office **252-744-2914** · Fax **252-744-2284** · rede.ecu.edu/umcirb/

Notification of Initial Approval: Expedited

From: Biomedical IRB
To: Sunghan Kim
CC:
Date: 11/4/2022
UMCIRB 22-001633
Re: GRAPH THEORETIC ANALYSIS OF THE HUMAN BRAIN'S FUNCTIONAL CONNECTIVITY ALTERATION DUE TO SLEEP RESTRICTION

I am pleased to inform you that your Expedited Application was approved. Approval of the study and any consent form(s) occurred on 11/3/2022. The research study is eligible for review under expedited category # 4,7. The Chairperson (or designee) deemed this study no more than minimal risk.

As the Principal Investigator you are explicitly responsible for the conduct of all aspects of this study and must adhere to all reporting requirements for the study. Your responsibilities include but are not limited to:

1. Ensuring changes to the approved research (including the UMCIRB approved consent document) are initiated only after UMCIRB review and approval except when necessary to eliminate an apparent immediate hazard to the participant. All changes (e.g. a change in procedure, number of participants, personnel, study locations, new recruitment materials, study instruments, etc.) must be prospectively reviewed and approved by the UMCIRB before they are implemented;

2. Where informed consent has not been waived by the UMCIRB, ensuring that only valid versions of the UMCIRB approved, date-stamped informed consent document(s) are used for obtaining informed consent (consent documents with the IRB approval date stamp are found under the Documents tab in the ePIRATE study workspace);

3. Promptly reporting to the UMCIRB all unanticipated problems involving risks to participants and others;

4. Submission of a final report application to the UMICRB prior to the expected end date provided in the IRB application in order to document human research activity has ended and to provide a timepoint in which to base document retention; and

5. Submission of an amendment to extend the expected end date if the study is not expected to be completed by that date. The amendment should be submitted 30 days prior to the UMCIRB approved expected end date or as soon as the Investigator is aware that the study will not be completed by that date.

The approval includes the following items:

Name	Description
Email template (1).docx	Recruitment Documents/Scripts
Informed Consent Document.doc	Consent Forms
SR_Questionnaire.docx	Surveys and Questionnaires
Thesis Proposal Draft.pdf	Study Protocol or Grant Application

For research studies where a waiver or alteration of HIPAA Authorization has been approved, the IRB states that each of the waiver criteria in 45 CFR 164.512(i)(1)(i)(A) and (2)(i) through (v) have been met. Additionally, the elements of PHI to be collected as described in items 1 and 2 of the Application for Waiver of Authorization have been determined to be the minimal necessary for the specified research.

The Chairperson (or designee) does not have a potential for conflict of interest on this study.

IRB00000705 East Carolina U IRB #1 (Biomedical) IORG0000418
IRB00003781 East Carolina U IRB #2 (Behavioral/SS) IORG0000418

___

Study.PI Name:
Study.Co-Investigators:

Appendix B: Informed Consent Document

East Carolina University

Informed Consent to Participate in Research

Information to consider before taking part in research that has no more than minimal risk.

Title of Research Study: Graph Theoretic Analysis the Human Brain's Functional Connectivity Alteration Due to Sleep Restriction

Principal Investigator: Sunghan Kim (Person in Charge of this Study)
Institution, Department or Division: Engineering
Address: 216 Slay, Greenville, NC 27858
Telephone #: (252)737-1750

Researchers at East Carolina University (ECU) study issues related to society, health problems, environmental problems, behavior problems and the human condition. To do this, we need the help of volunteers who are willing to take part in research.

Why am I being invited to take part in this research?

The purpose of this research is to study the differences in brain waves between normal controls and subjects who don't get enough sleep. These brain waves can be recorded from the surface of the scalp using a technique that displays a series of facial images. This research study is aiming to assess the reliability and consistency of the data analysis techniques used to pick up on the small differences in the subjects' response to presented facial images. You are being invited to take part in this research because you are 18-30 years of age. In addition, you are considered cognitively healthy. The decision to take part in this research is yours to make. By doing this research, we hope to learn how sensitive the analysis technique is to the small changes expected in brain waves due to lack of sleep.

If you volunteer to take part in this research, you will be one of about 20 people to do so.

Are there reasons I should not take part in this research?

You should not volunteer for this research study if you are under 18 years of age or greater than 30 years of age and/or on medication for depression, sleep disorders, psychotic disorders, or if you have a pacemaker or internal defibrillator. In addition, you should not volunteer for this study if you are visually impaired.

What other choices do I have if I do not take part in this research?

You can choose not to participate. There is no alternative.

Where is the research going to take place and how long will it last?

The research will be conducted at ECU Biomedical Instrumentation and Data Analysis Laboratory (Science and Technology Building 134). You will need to come to the examination room twice during the study. You will be asked to volunteer for approximately 1 hour per visit (2 hours in total).

What will I be asked to do?

You will be asked to do the following: The first task is to answer a brief questionnaire regarding your wellness before volunteering in the research study. Afterwards you will take around 2–minute Psychomotor Vigilance test (PVT). A graduate student researcher will then have you wear a cap with 32 electrodes while you are seated on a comfortable chair. Those electrodes will make direct contact with your scalp but should not cause any pain. The graduate student researcher will draw your attention to a monitor in front of you. The visual stimuli (i.e., images) will be displayed on the monitor screen. The images to be flashed on the screen will consist of two-classes of gray-scale images. The two classes of gray-scale images will consist of familiar faces such as famous actors, celebrities, and politicians, random objects including clocks or flowers. You will be asked to fixate your eyes on each of them. Meanwhile, a computer, to which the cap is connected, will be used to record your brain activity through the 32 electrodes attached to the cap.

After one week of the first screening, you'll be asked to get no more than 5 hours of sleep and go about your regular day while holding to several instructions to induce the mental fatigue state: (1) Avoid napping during the day of the second screening; (2) Avoid caffeinated drinks in all forms e.g., coffee, tea, or energy drinks; (3) Maintain your regular level of physical activity during the day; 4) Be within walking distance from the lab to avoid driving, as experiencing some form of fatigue at that time is probable.

After at least 8 hours, you'll be asked to come to the lab and perform the same PVT and brain activity recording.

What might I experience if I take part in the research?

We don't know of any risks (the chance of harm) associated with this research. Any risks that may occur with this research are no more than what you would experience in everyday life. We don't know if you will benefit from taking part in this study. There may not be any personal benefit to you but the information gained by doing this research may help others in the future.

Will I be paid for taking part in this research?

We will be able to pay you for the time you volunteer while being in this study. Each participant will receive a $50 Greenphire ClinCard upon completing the 2nd screening.

Will it cost me to take part in this research?

It will not cost you any money to be part of the research.

Who will know that I took part in this research and learn personal information about me?

ECU and the people and organizations listed below may know that you took part in this research and may see information about you that is normally kept private. With your permission, these people may use your private information to do this research:

- Any agency of the federal, state, or local government that regulates human research. This includes the Department of Health and Human Services (DHHS), the North Carolina Department of Health, and the Office for Human Research Protections.
- The University & Medical Center Institutional Review Board (UMCIRB) and its staff have responsibility for overseeing your welfare during this research and may need to see research records that identify you.
-

How will you keep the information you collect about me secure? How long will you keep it?

All individuals working on this study have received special training on protecting your privacy and keeping you research and health information confidential. You will be assigned a special identification number for this study instead of your name. No printed forms that have your name, aside from this consent form, will be kept by the research study team. All printed

forms will be shredded 6 years after study closure to protect your personal health information.

This research study will use computers to collect your brainwave recordings and data servers to store them. Computers will be password-protected so that only authorized people on the research team may use them. Any information taken will exclude personal identification. Data servers are securely managed by East Carolina University.

There will be no video or audio recordings made during your participation in this study. You will not be identified in any data analysis, report, or publication about this study. Although every effort will be made to keep research records private, there may possibly be times when federal or state law requires the disclosure of such records. This is very unlikely, but if disclosure is ever required, East Carolina University will take steps allowable by law to protect the privacy of your personal information.

What if I decide I don't want to continue in this research?

You can stop at any time after it has already started. There will be no consequences if you stop, and you will not be criticized. You will not lose any benefits that you normally receive.

Who should I contact if I have questions?

The people conducting this study will be able to answer any questions concerning this research, now or in the future. You may contact the Principal Investigator at (252) 737-1750 (Monday through Friday, 9:00 am - 5:00 pm).

If you have questions about your rights as someone taking part in research, you may call the University & Medical Center Institutional Review Board (UMCIRB) at phone number 252-744-2914 (days, 8:00 am-5:00 pm). If you would like to report a complaint or concern about this research study, you may call the Director for Human Research Protections, at 252-744-2914

Is there anything else I should know?

Your information or biospecimen collected as part of the research, even if identifiers are removed, will not be used or distributed for future studies.

I have decided I want to take part in this research. What should I do now?

The person obtaining informed consent will ask you to read the following and if you agree, you should sign this form:

- I have read (or had read to me) all the above information.
- I have had an opportunity to ask questions about things in this research I did not understand and have received satisfactory answers.
- I know that I can stop taking part in this study at any time.
- By signing this informed consent form, I am not giving up any of my rights.
- I have been given a copy of this consent document, and it is mine to keep.

Participant's Name (PRINT) **Signature** **Date**

Person Obtaining Informed Consent: I have conducted the initial informed consent process. I have orally reviewed the contents of the consent document with the person who has signed above, and answered all of the person's questions about the research.

Person Obtaining Consent (PRINT) **Signature** **Date**

Appendix C: Medical History Questionnaire

Questionnaire

Title of Research Study: Graph Theoretic Analysis of The Human Brain's Functional Connectivity Alteration Due to Sleep Restriction

Principal Investigator: Sunghan Kim (Person in Charge of this Study)
Institution, Department or Division: Department of Engineering, East Carolina University
Address: East 5th Street, Greenville, NC 27858
Telephone #: (252) 737-1750
Study Coordinator: Marwa Antar
Telephone #: (252) 737-1750

This is a questionnaire designed to gather information about you that can allow us to conclude whether you are fit for the study, whether the study involves risks for you to participate in, or whether the data we gather from you will be of sufficient quality. For each question below, please circle the answer that fits your description (YES or NO). If you do not believe that a question can be answered with a simple yes or no, write in your response beside the field labeled "other:".

Medical History

Have you ever been diagnosed with any sleep disorders?

YES NO
Other:_____

Have you ever been diagnosed with diabetes?

YES NO
Other:_____

Have you ever been diagnosed with any endocrine disorders?

YES NO
Other:_____

Have you ever been diagnosed with any psychiatric or neurological diseases?

YES NO
Other:_____

Do you have any form of cognitive impairment?

YES NO
Other:_____

Do you suffer from epilepsy or any ailment that can cause harm when presented with rapidly flashing or bright stimulus?

YES NO
Other:_____

Are you currently taking any neuroleptic medications?

YES NO
Other:_____

Is there anything else that the principal investigator and study coordinator should be aware of? (if so, please write it in the "other" section)

YES NO
Other:_____

Sleeping habits (for the past 4 weeks only)

On average, how many hours did you sleep each night?

0-4 hours 5-6 hours 7-8 hours 8-10 hours

How long did you usually nap?

0-30 minutes 60 minutes 90 minutes or more

Do you feel that your sleep was not quiet/relaxing (e.g. feeling tense, moving restlessly, can't get comfortable)?

Not at all Somewhat Most of the time All the time

Recent 24 Hours

Did you sleep at least six hours the previous night?

YES NO
Other:_____

Do you feel awake and alert?

YES NO
Other:_____

Have you eaten in the past 8 hours?

YES NO
Other:_____

Have you consumed any caffeinated beverages?

YES NO
Other:_____

Are you under the effects of any stimulants or medications intended to enhance focus (example: amphetamines for those diagnosed with attention deficit hyperactive disorder)?

YES NO
Other:_____

Are you under the effects of any substances or medications that may dull the ability to focus or concentrate (example: certain pain medications or barbiturates)?

YES NO
Other:_____